

**The Enhanced Finite State Projection algorithm, using
conditional moment closure and time-scale separation**

by

Ukjin Kwon

Submitted to the Department of Electrical Engineering and Computer
Science

in partial fulfillment of the requirements for the degree of
Master of Science in Electrical Engineering and Computer Science

at the

MASSACHUSETTS INSTITUTE OF TECHNOLOGY


June 2019

© Massachusetts Institute of Technology 2019. All rights reserved.



Signature redacted

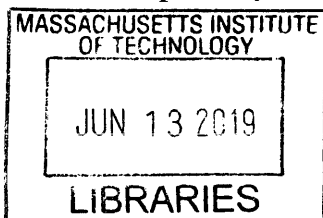
Author
Department of Electrical Engineering and Computer Science
May 22, 2019


Signature redacted

Certified by ...
 Domitilla Del Vecchio
Professor of Mechanical Engineering
Thesis Supervisor


Signature redacted

Accepted by
 Leslie A. Kolodziejcki
Professor of Electrical Engineering and Computer Science
Chair, Department Committee on Graduate Students



ARCHIVES



77 Massachusetts Avenue
Cambridge, MA 02139
<http://libraries.mit.edu/ask>

DISCLAIMER NOTICE

Due to the condition of the original material, there are unavoidable flaws in this reproduction. We have made every effort possible to provide you with the best copy available.

Thank you.

The images contained in this document are of the best quality available.

The Enhanced Finite State Projection algorithm, using conditional moment closure and time-scale separation

by

Ukjin Kwon

Submitted to the Department of Electrical Engineering and Computer Science
on May 22, 2019, in partial fulfillment of the
requirements for the degree of
Master of Science in Electrical Engineering and Computer Science

Abstract

The Chemical Master Equation (CME) is commonly used to describe the stochastic behavior of biomolecular systems. However, in general, the CME's dimension is very large or infinite, so analytical solutions may be difficult to achieve. To handle this problem, the Finite State Projection (FSP) algorithm can be used. However, when multiple time scales exist, which is common in biomolecular systems, the FSP algorithm also suffers from the computational issue. To deal with this problem, we propose the Enhanced Finite State Projection (EFSP) algorithm, which combines the original FSP algorithm and the model reduction technique that we developed, to approximate an infinite dimensional CME with a finite dimensional CME that contains the slow species only. We quantify the approximation error between the slow-species counts' marginal probability distribution of the original CME and those of the approximated CME, and prove that this error becomes smaller as δ (the EFSP error) or ε (time-scale separation between the fast and slow species) decreases. Unlike other time-scale separation methods, which rely on the fast-species counts' stationary conditional probability distributions, our model reduction technique relies on only the first few conditional moments of the fast-species counts. This is possible because we apply conditional moment closure to close the fast-species counts' dynamics, which provides a significant computation advantage. The benefit of our algorithm is illustrated through a protein binding reaction and a toggle switch.

Thesis Supervisor: Domitilla Del Vecchio
Title: Professor of Mechanical Engineering

Acknowledgments

My two years at MIT was the most diverse and meaningful time in my life in three different ways. I would like to take this opportunity to extend my sincerest gratitude.

First, I appreciate that MIT gave me an opportunity to learn and do research with the best resources. I always craved to study at MIT ever since I was a high school student. I could not forget the moment that I received an admission letter from MIT EECS department. During my undergraduate year, my goal was getting an admission from MIT, and I studied so hard in control theory and robotics field. Here at MIT, I am still studying control theory by taking high quality courses taught by wonderful faculty members, and applying it to synthetic biology, which I had never heard before I came to MIT. This field is very fascinating and control theorists can contribute a lot. In addition, MIT is the best place to conduct research in this field. I always appreciate this great opportunity.

Second, I appreciate that MIT gave me an opportunity to meet various smart people with passion and warm hearts. First and foremost, I would like to thank my advisor Prof. Domitilla Del Vecchio. She introduced me to synthetic biology field, which is highly interdisciplinary and vibrant field of research. Her enthusiasm and commitment to research give me a strong motivation. In addition, I respect her not only as an advisor but as a person, because she always considers students' situations when she gives us her opinion. I also want to appreciate my wonderful lab mates, including Heejin Ahn, Mohammad Naghnaeian and Penny Chen. I appreciate my friends, who give me positive energy and motivation. Also, I appreciate my parents, Kyoin Kwon and Hyeyoung Jung, who supported me unconditionally and wholeheartedly. Above all, Inyoung Kwon, my fiancé, has taken care of me for two years with a warm heart, encouragement and love. It would be impossible for me to easily settled in Cambridge without her. I am very excited to pursue my PhD and even further with her.

Third, I appreciate that I found another dream (other than receiving an admission letter from MIT) here at MIT. I want to make positive impact on the world by using my skill set that I have developed and the amazing people that I have met here. I can not decide what exactly I would want to do after I graduate, but there are so many different ways to achieve

my dream. I can be a professor or a researcher to conduct a novel research in synthetic biology field, or I can do my own start-up by using the skill set and all my connections. I could not find this dream without MIT, which always broadened my thinking and stimulated my heart.

Finally, I want to appreciate Korea Foundation for Advanced Studies (KFAS) and the Air Force Office of Scientific Research under grant FA9550-14-1-0060, who supported my tuition and stipend, so I could be fully focused on research.

Contents

1	Introduction	9
2	Preliminaries	13
3	Basic setup	17
4	Robust Conditional Moment Closure	21
5	Time-Scale Separation	25
6	Error Quantification	27
6.1	Conditional Moments of the Fast-Species Counts	27
6.2	Marginal Probability Distribution of the Slow-Species Counts	28
7	The FSP and the EFSP algorithms	31
7.1	The FSP algorithm in general	31
7.2	The EFSP algorithm where two time-scale exists	35
8	Examples	41
8.1	Protein Binding Reaction	41
8.2	Toggle Switch	46
9	conclusion	51
10	APPENDIX	53
10.1	Proof of Proposition 3.0.1 and 3.0.2	53

10.2 Iterative algorithm in Remark 4.0.1 54
10.3 Proof of Theorem 6.1.1 55
10.4 Proof of Lemma 6.2.1 57
10.5 Proof of Theorem 6.2.2 57
10.6 Proof of Corollary 6.2.3 58
10.7 Proof of Theorem 7.2.1 58

Chapter 1

Introduction

To analyze the behavior of biomolecular systems, deterministic or stochastic methods can be used [1]. At the single-cell level, the randomness of molecular events can have substantial repercussions on an emergent system's behavior. For example, fluctuations in gene expression are critical to phenotypic diversity in clonal populations [2][3][4]. Deterministic models fail to capture the inherent randomness of biomolecular systems, so stochastic approaches are often needed. The Chemical Master Equation (CME) gives the temporal description of the progression of a system's state probability distribution [5]. However, when the number of molecular counts is large or unbounded, the dimension of the CME is large or countably infinite. Therefore, analytical or computational solutions of the CME are very difficult to obtain in general.

To obtain sample paths that result from the CME, the Stochastic Simulation Algorithm (SSA) [6] is used. However, when the number of reactions increases or there is a large time-scale separation among reactions, this algorithm can become computationally expensive, resulting in long simulation time. To address the simulation time issue, Rao, Haseltine, and Gomez [7][8] [9] ran the SSA algorithm only with the slow reactions. These approaches require an approximation of the fast-species counts as a function of the slow-species counts. In particular, [7] approximated the stationary conditional probability distribution of the fast-species counts as functions of the slow-species counts. Obtaining the stationary conditional probability distribution of the fast-species counts is equivalent to obtaining the fast-species counts' stationary conditional moments of all different orders[10], and the number of con-

ditional moments grow exponentially with the number of the fast-species counts. Instead of using stationary conditional probability distribution, [9] used stationary distribution of the first n conditional moments of the fast-species counts. In this process, a moment closure technique was proposed to close the moments' dynamics. However, this moment closure technique does not provide a quantifiable approximation error bound. [8] approximated the dynamics of the fast-species counts through chemical Langevin equations, which are inaccurate when molecule counts are low.

Another way to address the CME's computational issue is to use the Finite State Projection (FSP) algorithm developed by Munsky et al. [11]. When the number of molecular counts is unbounded, the system's state space becomes an infinite set. The FSP algorithm finds an upper bound to the molecular count of each species and truncates the system's state space as a finite set, so that the truncated finite dimensional system's trajectories of probabilities are as close as desired to those of the original infinite dimensional CME. In several examples, the FSP algorithm outperformed SSA algorithms in terms of computational efficiency as well as accuracy [11]. However, when multiple time scales exist, the FSP algorithm also confronts a computational issue. This is because the algorithm equally treats the transition rates between states, even though they typically vary over several orders of magnitude [12].

To handle this problem, Peleš [12] combined the FSP algorithm and time-scale separation. In particular, Peleš applied the FSP algorithm to the approximated CME that contains the slow species only. To obtain the approximated CME with the slow species only, the author applied the time-scale separation technique developed by Khalil and Yin [13] [10], and approximated the stationary conditional probability distribution of the fast-species counts as functions of the slow-species counts as [7] did. However, the size of the vector of these stationary distributions grows exponentially with the number of the fast-species counts.

In this paper, we propose the Enhanced Finite State Projection (EFSP) algorithm, which combines the original FSP algorithm and the model reduction technique that we developed [14] to approximate an infinite dimensional CME with a finite dimensional CME, which contains the slow species only. Instead of considering the fast-species counts' stationary conditional probability distributions, our model reduction technique considers the first few

conditional moments of the fast-species counts, which provides a significant computation advantage. We assume that the number of fast-species counts is bounded, which is reasonable in many biomolecular systems of practical interest [5], but allow an unbounded number of slow-species counts.

For each iteration of the EFSP algorithm, we obtain the truncated state space of the slow species, which is a finite set. Then, we write Ordinary Differential Equations (ODEs) for both the marginal probability distribution of the slow-species counts, with the truncated state space at that iteration, and for the first n conditional moments of the fast-species counts. Here, n is an arbitrary (small) number, which gives a trade off between approximation accuracy and computational complexity. Next, we apply the conditional moment closure technique developed by Naghnaeian [15], time-scale separation and linear program to approximate the fast-species counts' first n conditional moments as functions of the slow-species counts. By substituting these functions in the ODEs that describe the marginal probability distribution of the slow-species counts, we can obtain a low dimensional CME with the slow species only. Therefore, for each iteration, unlike the original FSP algorithm, which relies on the solution of the full CME, the EFSP algorithm only relies on the solution of the approximated CME that contains the slow species only. This difference improves computational efficiency of the EFSP algorithm. In addition, different from [12], our method does not require the slow-species counts' stationary conditional probability distribution, which provides a significant computation advantage. The overall procedure of the EFSP algorithm is depicted in Fig. 1-1. We quantify the approximation error between the slow-species counts' marginal probability distribution of the original CME and those of the approximated CME. In particular, we can prove that this error becomes smaller as δ (the EFSP error) or ϵ (time-scale between the fast and slow species) decreases. We illustrate the application of this method to a protein binding reaction and a toggle switch.

This paper is organized as follows: in Section 2, we define mathematical notations and derive the CME used throughout this paper. In Section 3, we derive ODEs for the slow-species counts' marginal probability distribution and for the fast-species counts' first n conditional moments based on the CME. From Section 4 to 6, we introduce a model reduction technique. In particular, in Section 4, we apply the robust conditional moment

closure technique to close the dynamics of the fast-species counts. In Section 5, we apply time-scale separation and approximate the first n conditional moments of the fast-species counts as functions of the slow-species counts, and obtain an approximate CME with the slow species only. In Section 6, we derive the approximation error between the original CME and the approximated CME. In Section 7, we first introduce the FSP algorithm in general. Then we propose the EFSP algorithm. In Section 8, we illustrate the implementation of our method through two examples, a protein binding reaction and a toggle switch.

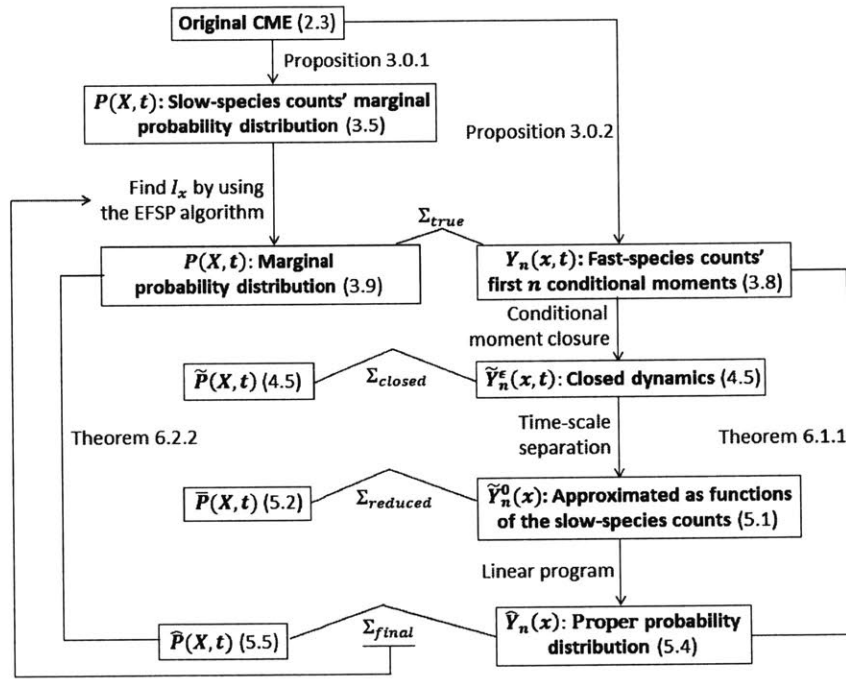


Figure 1-1: Schematic diagram illustrating overall procedure of the EFSP algorithm.

Chapter 2

Preliminaries

In this section, we define notations that are used throughout this paper. $\mathbb{Z}_{\geq 0}$ and $\mathbb{R}_{\geq 0}$ are the sets of nonnegative integers and real numbers, respectively. For any positive integer n , $\mathbb{Z}_{\geq 0}^n$ ($\mathbb{R}_{\geq 0}^n$) implies the set of n -dimensional vectors with each entry in $\mathbb{Z}_{\geq 0}$ ($\mathbb{R}_{\geq 0}$). Given a nonnegative integer w and an n -dimensional vector $Z = [z_1, z_2, \dots, z_n]^T$, we define $\Psi_w(Z)$ to be the vector made up of entries of the form $z_1^{k_1} z_2^{k_2} \dots z_n^{k_n}$ where $k_i \in \mathbb{Z}_{\geq 0}$, for $i = 1, 2, \dots, n$, and $\sum_{i=1}^n k_i = w$. For instance, when $Z = [z_1, z_2, z_3, z_4]$,

$$\begin{aligned} \Psi_1(Z) &= [z_1, z_2, z_3, z_4]^T, \\ \Psi_2(Z) &= [z_1^2, z_1 z_2, z_1 z_3, z_1 z_4, z_2^2, z_2 z_3, z_2 z_4, z_3^2, z_3 z_4, z_4^2]^T. \end{aligned} \tag{2.1}$$

The l_∞ and l_1 norms of a vector $Z = [z_1, z_2, \dots, z_n]^T$ are defined as $\|Z\|_\infty = \max_i |z_i|$ and $\|Z\|_1 = \sum_{i=1}^n |z_i|$, respectively. For the l_∞ norm, we eliminate the subscript ∞ and simply note $\|Z\|$. We call a vector $P \in \mathbb{R}_{\geq 0}^p$ a probability vector when $\|P\|_1 = 1$. The l_∞ induced norm of matrix M is defined as

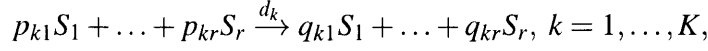
$$\|M\| = \max_i \sum_{j=1}^n |m_{ij}|.$$

The l_1 to l_∞ induced norm of matrix M is defined as $\|M\|_{l_1-l_\infty} = \max_{i,j} |m_{ij}|$. We define $\mathcal{R}[M]_i$ as the i^{th} row of $M = [m_{ij}] \in \mathbb{R}^{m \times n}$, which implies that

$$\mathcal{R}[M]_i = [m_{i1} \quad m_{i2} \quad \dots \quad m_{in}],$$

for $i = 1, 2, \dots, m$.

Now, we consider a biomolecular system with r species, S_1, \dots, S_r , and K reactions of the form:



where $q_{kl} - p_{kl}$ is the change in the number of molecules of S_l by the k^{th} reaction and d_k stands for the k^{th} reaction rate constant. Let s_i , for $i = 1, 2, \dots, r$, be the molecular count for each species as a discrete random variable and let $\mathbf{s} = [s_1, s_2, \dots, s_r]^T$ be the state of the system. Then, for any $\mathbf{s} \in \mathbb{Z}_{\geq 0}^r$, the Chemical Master Equation (CME) takes the form

$$\frac{\partial P(\mathbf{s}, t)}{\partial t} = \sum_{k=1}^K [-a_k(\mathbf{s})P(\mathbf{s}, t) + a_k(\mathbf{s} - \gamma_k)P(\mathbf{s} - \gamma_k, t)] \quad (2.2)$$

where γ_k is a stoichiometry vector and $a_k(\mathbf{s})$ is a propensity function. When we let $p_k = [p_{k1}, \dots, p_{kr}]^T$ and $q_k = [q_{k1}, \dots, q_{kr}]^T$, for $k = 1, 2, \dots, K$, then $\gamma_k = q_k - p_k$. $a_k(\mathbf{s})$ is proportional to d_k and $a_k(\mathbf{s})dt$ is the probability that the k^{th} reaction takes place in an infinitesimal time step dt [16] [17].

Let Ω_s be the state space of all species, which implies $\mathbf{s} \in \Omega_s$. Since Ω_s is a subset of a countable set $\mathbb{Z}_{\geq 0}^r$, it is also countable. Let $\{\mathbf{s}_i\} = \{\mathbf{s}_1, \mathbf{s}_2, \dots\}$ be an enumeration of Ω_s , and define $S = [\mathbf{s}_1, \mathbf{s}_2, \dots]^T$. Then according to Minsky [11], when we let

$$P(S, t) = [P(\mathbf{s}_1, t), P(\mathbf{s}_2, t), \dots]^T,$$

which is the probability density state vector at time t , (2.2) can be written as a single linear expression:

$$\frac{d}{dt}P(S, t) = MP(S, t), \quad \text{given } P(S, t_0), \quad (2.3)$$

where,

$$M_{ij} = \begin{cases} -\sum_{k=1}^K a_k(\mathbf{s}_j) & \text{if } i = j, \\ a_k(\mathbf{s}_j) & \text{if } \mathbf{s}_j = \mathbf{s}_i - \gamma_k, \\ 0 & \text{Otherwise.} \end{cases}$$

In this work, we consider biomolecular systems in which the chemical reactions take place on two time-scales. Let K_s be the number of slow reactions and K_f be the number

of fast reactions where $K_s + K_f = K$. We are using a small positive parameter $\varepsilon (\ll 1)$, which quantifies a time-scale separation between the slow and fast reactions. Then, we can separate propensity functions as slow reactions' propensity functions $a_k(\mathbf{s})$, for $k = 1, 2, \dots, K_s$, and fast reactions' propensity functions $a_k(\mathbf{s})$, for $k = K_s + 1, K_s + 2, \dots, K_s + K_f = K$. Based on the slow and fast reactions, we can define the slow and fast species as follow. Upon firing the fast reactions, slow species counts never change. On the other hand, for each fast species, there exists at least one fast reaction that changes the fast-species counts. According to Jayanthi and Contou [18] [19], there exists a proper linear coordinate transformation that identifies the slow and fast species in the system. Let X_1, \dots, X_l be the slow species and Y_1, \dots, Y_q be the fast species, where $l + q = r$. Let x_i , for $i = 1, 2, \dots, l$, y_j , for $j = 1, 2, \dots, q$, be the molecular count for each slow and fast species, respectively. Let $\mathbf{x} = [x_1, x_2, \dots, x_l]^T$ and $\mathbf{y} = [y_1, y_2, \dots, y_q]^T$ be the state of the system for each slow and fast species, respectively. Then $\mathbf{s} \in \mathbb{Z}_{\geq 0}^r$ can be represented as $\mathbf{s} = (\mathbf{x}, \mathbf{y})$, where $\mathbf{x} \in \mathbb{Z}_{\geq 0}^l$ stands for the slow-species counts and $\mathbf{y} \in \mathbb{Z}_{\geq 0}^q$ stands for the fast-species counts. In addition, for $k = 1, 2, \dots, K$, propensity function $a_k(\mathbf{s})$ can be written as $a_k(\mathbf{x}, \mathbf{y})$. Now we make the following assumptions:

Assumption 2.0.1. *There exist nonnegative integers y_{tot}^j such that*

$$0 \leq y_j \leq y_{tot}^j, \text{ for } j = 1, 2, \dots, q.$$

Assumption 2.0.2. *All of the propensity functions are polynomial in \mathbf{s} [16]. In addition, the order of each polynomial is less than or equal to 2.*

Assumption 2.0.1 requires that the number of fast species is bounded, which is reasonable in many biomolecular systems of practical interest. For example, in gene regulatory network models, the fast species are usually complexes formed by transcription factors with DNA, which are in finite amount [5]. Gillespie derived that propensity functions are polynomial under suitable conditions such as well-mixedness [16]. Assumption 2.0.2 states that the order of each polynomial for the propensity function is at most two because reactions are either uni-molecular or bi-molecular. This is a standard assumption considering that n -molecular reactions ($n > 2$) have low probability compared to a sequence of bi-molecular

reactions [5]. In addition, propensity functions can be written as follows [14] [15]:

$$\begin{aligned}
a_k(\mathbf{x}, \mathbf{y}) &= b_k(\mathbf{x}) + c_k(\mathbf{x})\Psi_1(\mathbf{y}) + d_k\Psi_2(\mathbf{y}), \text{ for } k = 1, 2, \dots, K_s, \\
a_k(\mathbf{x}, \mathbf{y}) &= \frac{1}{\varepsilon}(b_k(\mathbf{x}) + c_k(\mathbf{x})\Psi_1(\mathbf{y}) + d_k\Psi_2(\mathbf{y})), \\
&\text{for } k = K_s + 1, 2, \dots, K,
\end{aligned} \tag{2.4}$$

where $\Psi_1(\mathbf{y})$ and $\Psi_2(\mathbf{y})$ are defined in (2.1). $b_k(\mathbf{x})$ is a polynomial in \mathbf{x} with order less than or equal to 2. $c_k(\mathbf{x})$ is a matrix with appropriate dimensions, and each component of $c_k(\mathbf{x})$ is a polynomial in \mathbf{x} with order less than or equal to 1. d_k is a constant matrix with appropriate dimension. The propensity functions of the slow reactions are an order of ε of the propensity functions of the fast reactions.

We let Ω_x and Ω_y , be the state space of the slow species and the fast species, respectively. Since each slow-species counts is unbounded, $\Omega_x = \mathbb{Z}_{\geq 0}^l$. On the other hand, because of Assumption 2.0.1, $\Omega_y \subset \mathbb{Z}_{\geq 0}^q$ and it is a finite set. Then \mathbf{x} and \mathbf{y} will be vectors of random variables taking values in the sets Ω_x and Ω_y , respectively. Then, $\Omega_s = \Omega_x \times \Omega_y$, which is a subset of $\mathbb{Z}_{\geq 0}^r$. Ω_y is a countable set because it is a finite set, and Ω_x is also a countable set because it is a finite product of countable sets. Let $\{\mathbf{x}_i\}$ and $\{\mathbf{y}_j\}$ be an enumeration of Ω_x and Ω_y , respectively.

Then for any $\mathbf{x} \in \Omega_x$ and $\mathbf{y} \in \Omega_y$, we can rewrite the CME as

$$\begin{aligned}
\frac{d}{dt}P(\mathbf{x}, \mathbf{y}, t) &= \sum_{k=1}^{K_s} [-a_k(\mathbf{x}, \mathbf{y})P(\mathbf{x}, \mathbf{y}, t) \\
&+ a_k(\mathbf{x} - \gamma_{x,k}, \mathbf{y} - \gamma_{y,k})P(\mathbf{x} - \gamma_{x,k}, \mathbf{y} - \gamma_{y,k}, t)] \\
&+ \sum_{k=K_s+1}^K [-a_k(\mathbf{x}, \mathbf{y})P(\mathbf{x}, \mathbf{y}, t) + a_k(\mathbf{x}, \mathbf{y} - \gamma_{y,k})P(\mathbf{x}, \mathbf{y} - \gamma_{y,k}, t)],
\end{aligned} \tag{2.5}$$

where, for $k = 1, 2, \dots, K$, $a_k(\mathbf{x}, \mathbf{y})$ are propensity functions for the slow and fast reactions defined in (2.4), and $\gamma_{x,k}$ and $\gamma_{y,k}$ are corresponding stoichiometry vectors, for the slow species and the fast species, respectively [9]. For the fast reactions ($k = K_s + 1, \dots, K$), $\gamma_{x,k}$ is 0, because the slow-species counts are not changed by the fast reactions.

Chapter 3

Basic setup

In this section, we define ODEs for the slow-species counts' marginal probability distribution, $P(\mathbf{x}, t)$, and for the fast-species counts' first n conditional moments, $Y_n(\mathbf{x}, t)$, based on (2.5). To proceed, we define $P(\mathbf{y}, t|\mathbf{x})$ as the conditional probability distribution of the fast-species counts given the slow-species counts. Then, these two distributions, $P(\mathbf{x}, t)$ and $P(\mathbf{y}, t|\mathbf{x})$, jointly specify the full distribution $P(\mathbf{s}, t) = P(\mathbf{x}, \mathbf{y}, t)$ via

$$P(\mathbf{x}, \mathbf{y}, t) = P(\mathbf{x}, t)P(\mathbf{y}, t|\mathbf{x}),$$

by Bayes' theorem. Then we define

$$\begin{aligned}\mu_w(\mathbf{x}, t) &= \mathbb{E}[\Psi_w(Y)|\mathbf{x}] = \sum_{\mathbf{y} \in \Omega_y} \Psi_w(\mathbf{y})P(\mathbf{y}, t|\mathbf{x}), \\ Y_n(\mathbf{x}, t) &= [\mu_1(\mathbf{x}, t)^T, \mu_2(\mathbf{x}, t)^T, \dots, \mu_n(\mathbf{x}, t)^T]^T,\end{aligned}\tag{3.1}$$

for any $\mathbf{x} \in \Omega_x$, $w \in \mathbb{Z}_{\geq 0}$, $1 \leq n \leq |\Omega_y|$, where $\mu_w(\mathbf{x}, t)$ and $Y_n(\mathbf{x}, t)$ denote the fast-species counts' w^{th} and first n conditional moments, respectively. For $w = 1, 2, \dots, n$, let f_w be a matrix whose multiplication with $Y_n(\mathbf{x}, t)$ isolates $\mu_w(\mathbf{x}, t)$, i.e.,

$$\mu_w(\mathbf{x}, t) = f_w Y_n(\mathbf{x}, t).\tag{3.2}$$

Now we can derive ODEs from (2.5) for the slow-species counts' marginal probability distribution, $P(\mathbf{x}, t)$, as in (3.3):

Proposition 3.0.1. *For the CME in (2.5) with Assumptions 2.0.1 and 2.0.2, given $\mathbf{x} \in \Omega_x$, we have*

$$\begin{aligned} \frac{d}{dt}P(\mathbf{x}, t) &= \sum_{k=1}^{K_s} [-\mathbb{E}[a_k(\mathbf{x}, \mathbf{y})|\mathbf{x}]P(\mathbf{x}, t) \\ &+ \mathbb{E}[a_k(\mathbf{x} - \gamma_{x,k}, \mathbf{y})|\mathbf{x} - \gamma_{x,k}]P(\mathbf{x} - \gamma_{x,k}, t)]. \end{aligned} \quad (3.3)$$

The proof of Proposition 3.0.1 is in the Appendix. By using (2.4), we can further express the conditional expectation of propensity function $a_k(\mathbf{x}, \mathbf{y})$ as

$$\begin{aligned} \mathbb{E}[a_k(\mathbf{x}, \mathbf{y})|\mathbf{x}] &= \sum_{\mathbf{y}} a_k(\mathbf{x}, \mathbf{y})P(\mathbf{y}, t|\mathbf{x}) \\ &= b_k(\mathbf{x}) + c_k(\mathbf{x})\mu_1(\mathbf{x}, t) + d_k\mu_2(\mathbf{x}, t), \end{aligned} \quad (3.4)$$

for given \mathbf{x} and $1 \leq k \leq K_s$. When we let $X = [\mathbf{x}_1, \mathbf{x}_2, \dots]^T$, according to Munsky [11], the slow-species counts' marginal probability distribution in (3.3) can be written as a single linear expression:

$$\frac{d}{dt}P(X, t) = A(Y_2(\mathbf{x}, t))P(X, t), \text{ given } P(X, t_0), \quad (3.5)$$

where,

$$P(X, t) = [P(\mathbf{x}_1, t), P(\mathbf{x}_2, t), \dots, P(\mathbf{x}_i, t), \dots]^T \quad (3.6)$$

is the slow-species counts' marginal probability distribution vector at time t and

$$A_{ij} = \begin{cases} -\sum_{k=1}^{K_s} \mathbb{E}[a_k(\mathbf{x}_j, \mathbf{y})|\mathbf{x}_j] & \text{if } i = j, \\ \mathbb{E}[a_k(\mathbf{x}_j, \mathbf{y})|\mathbf{x}_j] & \text{if } \mathbf{x}_j = \mathbf{x}_i - \gamma_{x,k}, 1 \leq k \leq K_s, \\ 0 & \text{Otherwise.} \end{cases} \quad (3.7)$$

We can also derive ODEs from (2.5) for the fast-species counts' first n conditional moments, $Y_n(\mathbf{x}, t)$, as in (3.8):

Proposition 3.0.2. *For the CME in (2.5) with Assumptions 2.0.1 and 2.0.2, for $\mathbf{x} \in \Omega_x$ and*

$1 \leq n \leq |\Omega_y|$, we have

$$\varepsilon \frac{d}{dt} Y_n(\mathbf{x}, t) = C(\mathbf{x}) Y_n(\mathbf{x}, t) + c_1(\mathbf{x}) + c_2 \mu_{n+1}(\mathbf{x}, t) + \varepsilon G(t). \quad (3.8)$$

The proof of Proposition 3.0.2 is in the Appendix. For given $\mathbf{x} \in \Omega_x$ and $1 \leq n \leq |\Omega_y|$, let Σ_{true} be

$$\Sigma_{true} : \begin{cases} \frac{d}{dt} P(X, t) = [A(Y_2(\mathbf{x}, t))] P(X, t), \\ \varepsilon \frac{d}{dt} Y_n(\mathbf{x}, t) = C(\mathbf{x}) Y_n(\mathbf{x}, t) + c_1(\mathbf{x}) \\ \quad + c_2 \mu_{n+1}(\mathbf{x}, t) + \varepsilon G(t). \end{cases} \quad (3.9)$$

When $n = |\Omega_y|$, Σ_{true} is closed, because $\mu_{n+1}(\mathbf{x}, t)$ can be represented as an affine function of $Y_n(\mathbf{x}, t)$ [9]. However, in general, when $1 \leq n < |\Omega_y|$, the dynamics of the fast-species counts' conditional moments are not closed, because $\mu_{n+1}(\mathbf{x}, t)$ is not a function of $Y_n(\mathbf{x}, t)$ anymore. To solve this problem, we apply a robust conditional moment closure method to approximate $\mu_{n+1}(\mathbf{x}, t)$ as a function of $Y_n(\mathbf{x}, t)$ to close the dynamics. The next section proposes the robust moment closure technique developed by Naghnaeian [15], and it can be applied to the conditional moments.

Chapter 4

Robust Conditional Moment Closure

The Robust Moment Closure (RMC) was originally developed by Naghnaeian [15] for the moments dynamics. Here we modify it so to make it applicable to the dynamics of the conditional moments. For any $\mathbf{x} \in \Omega_x$, we define the fast-species counts' conditional probability distribution as

$$P_{Y|X}(\mathbf{x}, t) = [P(\mathbf{y}_1, t|\mathbf{x}), \dots, P(\mathbf{y}_j, t|\mathbf{x}), \dots, P(\mathbf{y}_{|\Omega_y|}, t|\mathbf{x})]^T.$$

Then for each $\mu_{n+1}(\mathbf{x}, t)$ and $Y_n(\mathbf{x}, t)$, there exists unique H_n and V_n that satisfy

$$\mu_{n+1}(\mathbf{x}, t) = H_n P_{Y|X}(\mathbf{x}, t), Y_n(\mathbf{x}, t) = V_n P_{Y|X}(\mathbf{x}, t).$$

For example, when $q = 1$,

$$H_n = \begin{bmatrix} 0 & 1^{n+1} & 2^{n+1} & \dots & (|\Omega_y|)^{n+1} \end{bmatrix}, \quad (4.1)$$

$$V_n = \begin{bmatrix} 0 & 1 & 2 & \dots & |\Omega_y| \\ 0 & 1^2 & 2^2 & \dots & |\Omega_y|^2 \\ \vdots & \vdots & & & \\ 0 & 1^n & 2^n & \dots & |\Omega_y|^n \end{bmatrix}. \quad (4.2)$$

Our objective is to approximate $\mu_{n+1}(\mathbf{x}, t)$ as a function of $Y_n(\mathbf{x}, t)$, so that (3.9) becomes closed, denoted as

$$\mu_{n+1}(\mathbf{x}, t) \approx \phi(Y_n(\mathbf{x}, t)),$$

where $\phi(\cdot)$ can be a nonlinear function. Since the conditional probability distribution, $P_{Y|X}(\mathbf{x}, t)$, is not known, $\phi(\cdot)$ should be chosen such that the worst-case error between $\mu_{n+1}(\mathbf{x}, t)$ and $\phi(Y_n(\mathbf{x}, t))$ is minimized. Therefore, the following min-max problem:

$$\inf_{\phi} \sup_{P_{Y|X}(\mathbf{x}, t) \in \mathbb{P}} \|\mu_{n+1}(\mathbf{x}, t) - \phi(Y_n(\mathbf{x}, t))\|, \quad (4.3)$$

should be solved. Naghnaeian [15] proved that without a priori information on the conditional probability distribution, $P_{Y|X}(\mathbf{x}, t)$, a solution for (4.3) is obtained when $\phi(Y_n(\mathbf{x}, t))$ is an affine function of $Y_n(\mathbf{x}, t)$, which can be written as

$$\phi(Y_n(\mathbf{x}, t)) = KY_n(\mathbf{x}, t) + K_0.$$

In addition, we can obtain K and K_0 by solving the linear program

$$\begin{aligned} \min_{K_0, K} \quad & \gamma \\ \text{s.t.} \quad & -\gamma \mathbf{1}^T \leq \mathcal{R}[H_n - (KV_n + K_0 \mathbf{1}^T)]_i \leq \gamma \mathbf{1}^T \end{aligned} \quad (4.4)$$

for $i = 1, 2, \dots, p$, where p is the number of rows in H_n . Let the linear program in (4.4)'s object value be ρ_n . When n is fixed, ρ_n is a constant. Then

$$\|\mu_{n+1}(\mathbf{x}, t) - \phi(Y_n(\mathbf{x}, t))\| = \|H_n P_{Y|X}(\mathbf{x}, t) - (KV_n P_{Y|X}(\mathbf{x}, t) + K_0)\|,$$

which is the approximation error between $\mu_{n+1}(\mathbf{x}, t)$ and $\phi(Y_n(\mathbf{x}, t))$, is bounded by ρ_n for any $P_{Y|X}(\mathbf{x}, t)$. On the right-hand side of Σ_{true} , we substitute $KY_n(\mathbf{x}, t) + K_0$ for $\mu_{n+1}(\mathbf{x}, t)$, and obtain

$$\Sigma_{closed} : \begin{cases} \frac{d}{dt} \tilde{P}(X, t) = [A(\tilde{Y}_2^\varepsilon(\mathbf{x}, t))] \tilde{P}(X, t) = \tilde{A}(t) \tilde{P}(X, t) \\ \varepsilon \frac{d}{dt} \tilde{Y}_n^\varepsilon(\mathbf{x}, t) = C(\mathbf{x}) \tilde{Y}_n^\varepsilon(\mathbf{x}, t) + c_1(\mathbf{x}) \\ + c_2(K \tilde{Y}_n^\varepsilon(\mathbf{x}, t) + K_0) + \varepsilon G(t). \end{cases} \quad (4.5)$$

Let us define $\tilde{\mu}_w^\varepsilon(\mathbf{x}, t) = f_w \tilde{Y}_n^\varepsilon(\mathbf{x}, t)$.

Remark 4.0.1. According to Lemma 10.3.1, if $C(\mathbf{x}) + c_2K$ is a stable matrix, that is, all of its eigenvalues have negative real part, the approximation error between $\mu_w(\mathbf{x}, t)$ and $\tilde{\mu}_w^\varepsilon(\mathbf{x}, t)$ is bounded. Even though the stability of $C(\mathbf{x}) + c_2K$ is not guaranteed in general via (4.4), we prove that this matrix is indeed stable in our examples. To ensure the stability

by construction, we can augment (4.4) with a linear matrix inequality and conduct an iterative algorithm. This procedure is in the Appendix. Here we assume that $C(\mathbf{x}) + c_2K$ is a stable matrix.

Chapter 5

Time-Scale Separation

We can check that (4.5) is written in standard singular perturbation form [13]. Let $\tilde{Y}_n^0(\mathbf{x})$ be the solution of

$$C(\mathbf{x})\tilde{Y}_n^0(\mathbf{x}) + c_1(\mathbf{x}) + c_2(K\tilde{Y}_n^0(\mathbf{x}) + K_0) = 0, \quad (5.1)$$

which can be obtained by letting $\varepsilon = 0$ in (4.5). Since $C(\mathbf{x}) + c_2K$ is a stable matrix, $\tilde{Y}_n^\varepsilon(\mathbf{x}, t)$ converges exponentially fast to $\tilde{Y}_n^0(\mathbf{x})$ [13]. By replacing $\tilde{Y}_2^\varepsilon(\mathbf{x}, t)$ with $\tilde{Y}_2^0(\mathbf{x})$ on the right-hand side of (4.5), we can obtain

$$\Sigma_{reduced} : \left\{ \frac{d}{dt} \bar{P}(X, t) = [A(\tilde{Y}_2^0(\mathbf{x}))] \bar{P}(X, t) = \bar{A} \bar{P}(X, t). \right. \quad (5.2)$$

$\Sigma_{reduced}$ is composed of the slow species only, because we approximate the conditional moments of the fast-species counts, $\tilde{Y}_2^\varepsilon(\mathbf{x}, t)$, as functions of the slow-species counts, $\tilde{Y}_2^0(\mathbf{x})$. $\Sigma_{reduced}$ is a positive system if and only if \bar{A} is a Metzler matrix [20]. However, this is not guaranteed in general. Because of (3.4) and (3.7), any off-diagonal element of \bar{A} has the form

$$b_k(\mathbf{x}) + c_k(\mathbf{x})\tilde{\mu}_1^0(\mathbf{x}) + d_k\tilde{\mu}_2^0(\mathbf{x}), \quad (5.3)$$

where $\tilde{\mu}_w^0(\mathbf{x}) = f_w\tilde{Y}_n^0(\mathbf{x})$, for $w = 1, 2$. Therefore, \bar{A} is a Metzler matrix if and only if (5.3) is non-negative for all $\mathbf{x} \in \Omega_x$. For given $\mathbf{x} \in \Omega_x$ and $k = 1, 2, \dots, K_s$, we define a linear

program

$$\begin{aligned} \min_{h_1(\mathbf{x}), h_2(\mathbf{x})} \quad & \|h_1(\mathbf{x}) - \tilde{\mu}_1^0(\mathbf{x})\| + \|h_2(\mathbf{x}) - \tilde{\mu}_2^0(\mathbf{x})\| \\ \text{s.t.} \quad & b_k(\mathbf{x}) + c_k(\mathbf{x})h_1(\mathbf{x}) + d_k h_2(\mathbf{x}) \geq 0. \end{aligned} \quad (5.4)$$

Let the optimal solution to (5.4) be $h_1(\mathbf{x}) = \hat{\mu}_1(\mathbf{x})$ and $h_2(\mathbf{x}) = \hat{\mu}_2(\mathbf{x})$ and the object value be $\lambda^{\mathbf{x}}$. By replacing $\tilde{\mu}_1^0(\mathbf{x})$ and $\tilde{\mu}_2^0(\mathbf{x})$ with $\hat{\mu}_1(\mathbf{x})$ and $\hat{\mu}_2(\mathbf{x})$ in $\Sigma_{reduced}$, we obtain

$$\Sigma_{final} : \left\{ \frac{d}{dt} \hat{P}(X, t) = [A(\hat{Y}_2(\mathbf{x}))] \hat{P}(X, t) = \hat{A} \hat{P}(X, t), \right. \quad (5.5)$$

where $\hat{Y}_2(\mathbf{x}) = [\hat{\mu}_1(\mathbf{x})^T, \hat{\mu}_2(\mathbf{x})^T]^T$. In (5.5), Σ_{final} is a positive system because \hat{A} is a Metzler matrix, which is guaranteed by (5.4). Furthermore, \hat{A} is a stable matrix and both $\|\hat{\mu}_1(\mathbf{x}) - \tilde{\mu}_1^0(\mathbf{x})\|$ and $\|\hat{\mu}_2(\mathbf{x}) - \tilde{\mu}_2^0(\mathbf{x})\|$ are bounded by $\lambda^{\mathbf{x}}$.

Remark 5.0.1. When $n = |\Omega_y|$, both ρ_n and $\lambda^{\mathbf{x}}$ are 0.

Proof. ρ_n is 0 because $\mu_{n+1}(\mathbf{x}, t)$ can be represented as an affine function of $Y_n(\mathbf{x}, t)$. $\lambda^{\mathbf{x}} = 0$ is proved by Gomez [9]. □

Now the approximation errors for both the fast-species counts' conditional moments and the slow-species counts' marginal probability distribution should be quantified.

Chapter 6

Error Quantification

6.1 Conditional Moments of the Fast-Species Counts

Here, we first consider the fast-species counts' conditional moments. The following theorem derives the approximation error between the fast-species counts' conditional moments of Σ_{true} , $\mu_w(\mathbf{x}, t)$, and those of Σ_{final} , $\hat{\mu}_w(\mathbf{x})$.

Theorem 6.1.1. *Given $t_f > t_0 > 0$ and $\mathbf{x} \in \Omega_x$, the approximation error between $\mu_w(\mathbf{x}, t)$ and $\hat{\mu}_w(\mathbf{x})$ satisfies*

$$\sup_{t \in [t_0, t_f]} \|\mu_w(\mathbf{x}, t) - \hat{\mu}_w(\mathbf{x})\| \leq \Delta_{w, \varepsilon}^{\mathbf{x}} + \lambda^{\mathbf{x}} + O(\varepsilon),$$

for $w = 1, 2$, where,

$$\Delta_{w, \varepsilon}^{\mathbf{x}} = \int_{t_0}^{t_f} \|f_w \exp\{\frac{1}{\varepsilon}(C(\mathbf{x}) + c_2 K)(t_f - \tau)\}\| d\tau \frac{\rho_n}{\varepsilon} \|c_2\|.$$

Furthermore, there exist $\Delta_\varepsilon > 0$ and $\varepsilon^* > 0$ such that $\sup_{t \in [t_0, t_f]} \|\mu_w(\mathbf{x}, t) - \hat{\mu}_w(\mathbf{x})\| \leq \Delta_\varepsilon + O(\varepsilon)$ for all \mathbf{x} , $\varepsilon \in (0, \varepsilon^*)$ and $w = 1$ or 2 .

The proof of Theorem 6.1.1 is presented in the Appendix together with several lemmas that are used in the proof. We provide an outline of the proof here. First, we derive the approximation error between the fast-species counts' conditional moments of Σ_{true} and those of Σ_{closed} . Then we derive the error between the fast-species counts' conditional moments of Σ_{closed} and those of $\Sigma_{reduced}$. The approximation error between the fast-species counts'

conditional moments of $\Sigma_{reduced}$ and those of Σ_{final} is derived by (5.4), which is λ^x . By combining these three results, using triangular inequality, we can obtain the approximation error between the fast-species counts' conditional moments of Σ_{true} , $\mu_w(\mathbf{x}, t)$, and those of Σ_{final} , $\hat{\mu}_w(\mathbf{x})$.

6.2 Marginal Probability Distribution of the Slow-Species Counts

Next, we quantify the approximation error of the slow-species counts' marginal probability distribution by using Theorem 6.1.1. In Σ_{final} , we construct a positive system by making \hat{A} Metzler and stable matrix. Now, let us regard Σ_{final} as our nominal system and (3.5) as the perturbed system. Then we can express the perturbed system as follows:

$$\frac{d}{dt}P(X, t) = (\hat{A} + \Delta_1(t))P(X, t), \quad (6.1)$$

where

$$\Delta_1(t) = [A(Y_2(\mathbf{x}, t))] - \hat{A}.$$

By using Theorem 6.1.1, we can prove that $l_1 - l_\infty$ norm of $\Delta_1(t)$ is bounded.

Lemma 6.2.1. *There is a constant k_1 such that*

$$\|\Delta_1(t)\|_{l_1 - l_\infty} \leq k_1 \Delta_\varepsilon + O(\varepsilon),$$

where Δ_ε is defined in Theorem 6.1.1.

The proof of Lemma 6.2.1 is in the Appendix. Now we can quantify the approximation error between the slow-species counts' marginal probability distribution of Σ_{true} , $P(X, t)$, and those of Σ_{final} , $\hat{P}(X, t)$, as follows:

Theorem 6.2.2. *Given $t_f > t_0 > 0$, the approximation error between $P(X, t)$ and $\hat{P}(X, t)$ satisfies*

$$\begin{aligned} & \sup_{t \in [t_0, t_f]} \|P(X, t) - \hat{P}(X, t)\| \\ & \leq k_1 \int_{t_0}^{t_f} \|\exp\{\hat{A}\}(t_f - \tau)\| d\tau \Delta_\varepsilon + O(\varepsilon). \end{aligned}$$

The proof of Theorem 6.2.2 is in the Appendix.

Corollary 6.2.3. *As $\varepsilon \rightarrow 0$, the right-hand side of the inequality in Theorem 6.2.2 goes to $k\Delta_0$, where*

$$\begin{aligned} k &= k_1 \int_{t_0}^{t_f} \|\exp\{\hat{A}(t_f - \tau)\}\| d\tau, \Delta_0 = \lim_{\varepsilon \rightarrow 0} \Delta_\varepsilon = \sup_{w \in \{1, 2\}, \mathbf{x} \in \Omega_x^t} (\Delta_{w,0}^{\mathbf{x}} + \lambda^{\mathbf{x}}), \text{ and} \\ \Delta_{w,0}^{\mathbf{x}} &= \lim_{\varepsilon \rightarrow 0} \Delta_{w,\varepsilon}^{\mathbf{x}} = \int_0^\infty \|f_w \exp\{(C(\mathbf{x}) + c_2 K)t\}\| dt \rho_n \|c_2\|. \end{aligned}$$

The proof of Corollary 6.2.3 is in the Appendix.

Remark 6.2.4. *When $n = |\Omega_y|$, the right-hand side of the inequality in Theorem 6.2.2 goes to $O(\varepsilon)$. This is because when $n = |\Omega_y|$, both ρ_n and $\lambda^{\mathbf{x}}$ go to 0 by Remark 5.0.1, so Δ_ε goes to 0.*

Remark 6.2.4 shows that when $n = |\Omega_y|$, the only error that remains will be due to time-scale separation. In addition, as $\varepsilon \rightarrow 0$, $\|P(X, t) - \hat{P}(X, t)\|$ goes to 0. Now we should find I_x , by using the EFSP algorithm, which is illustrated in Section 7.2, to approximate infinite dimensional CME as a finite dimensional CME, that contains the slow species only and sufficiently close to the original CME.

Chapter 7

The FSP and the EFSP algorithms

In this section, we first illustrate the FSP algorithm developed by Munsy[11] in general, for (2.2) and (2.3). Then we propose the EFSP algorithm which can be applied to (5.5), where two time-scale exists.

7.1 The FSP algorithm in general

Consider (2.3), which has the infinite state space $\Omega_s = \{\mathbf{s}_1, \mathbf{s}_2, \mathbf{s}_3, \dots\}$. Let $I = \{i_1, i_2, \dots, i_m\}$ denote a finite ordered index set. Then, for given I , we can define a truncated finite state space, Ω_s^I , as follows:

$$\Omega_s^I = \{\mathbf{s}_{i_1}, \mathbf{s}_{i_2}, \dots, \mathbf{s}_{i_m}\}.$$

For any matrix A and given ordered index set I , let A_I denote the principal submatrix of A , in which both rows and columns have been chosen and ordered according to I . For

example, when $A = \begin{bmatrix} 1 & 2 & 3 & 4 \\ 5 & 6 & 7 & 8 \\ 9 & 10 & 11 & 12 \\ 13 & 14 & 15 & 16 \end{bmatrix}$, $I = \{2, 3\}$, then $A_I = \begin{bmatrix} 6 & 7 \\ 10 & 11 \end{bmatrix}$. In addition, for

any vector X , X_I is the vector of those elements of X indexed by I . For example, when $X = [0.3, 0.7, 0.1, 1.1]^T$, $I = \{3, 2\}$, then $X_I = [0.1, 0.7]^T$. Based on (2.3), and a given finite

ordered index set I , we define $P^I(S, t)$ as solutions of

$$\frac{d}{dt}P^I(S, t) = M_I P^I(S, t), P^I(S, t_0) = P_I(S, t_0), \quad (7.1)$$

where $P^I(S, t)$ is the approximated finite dimensional probability distribution. The FSP algorithm provides a systematic method to find a finite ordered index set I , so that the approximated probability distribution, $P^I(S, t)$ in (7.1), is sufficiently close to the original infinite-dimensional probability distribution, $P(S, t)$. In particular, the solution of (7.1) for $t \in [t_0, t_f]$ is

$$P^I(S, t) = \exp(M_I t) P^I(S, t_0).$$

According to [11], for any pair of index sets, $I_1 \subset I_2$,

$$[\exp(M_{I_2})]_{I_1} \geq \exp(M_{I_1}) \geq 0. \quad (7.2)$$

Since the probability density vector $P(S, t)$ is always non-negative, (7.2) guarantees that

$$[\exp(M_{I_2} t_f)]_{I_1} P^{I_1}(S, t_0) \geq \exp(M_{I_1} t_f) P^{I_1}(S, t_0). \quad (7.3)$$

This result assures that when we gradually expand ordered index set I_j (as $I_1 \subset I_2 \dots \subset I_j \dots$), the approximation monotonically improves.

In addition, for given $\delta > 0$, $t_f \geq 0$ and I , if

$$\|\exp(M_I t_f) P^I(S, t_0)\|_{I_1} = \mathbf{1}^T [\exp(M_I t_f) P^I(S, t_0)] \geq 1 - \delta, \quad (7.4)$$

then

$$\exp(M_I t_f) P^I(S, t_0) \leq P_I(S, t_f) \leq \exp\{(M_I) t_f\} P^I(S, t_0) + \delta \mathbf{1} \quad (7.5)$$

is guaranteed [11]. (7.4) and (7.5) imply that the approximate solution, $P^I(S, t_f) = \exp(M_I t_f) P^I(S, t_0)$ never exceeds the actual solution, $P_I(S, t_f)$, and $\|P_I(S, t_f) - P^I(S, t_f)\| \leq \delta$, when (7.4) is satisfied.

We can depict the underlying idea of the FSP algorithm, by representing all possible

states as nodes on an infinite r -dimensional integer lattice, where r is the number of species in the biomolecular system and each node corresponds to distinct state, \mathbf{s}_i . Fig. 7-1 (Top) shows a lattice for $r = 2$. Here, we project this infinite lattice onto the finite subset enclosed by the gray square, that corresponds to an index set I . This projected state space is shown in Fig. 7-1 (Bottom), where I represents the truncated state space, and I' represents the complement of I , where I' is aggregated to a single point. (7.1) illustrates the truncated CME with the index set I . (7.1) reflects transitions between states within I as well as reactions that starts from I and end in I' . However, the equation ignores reactions that begin in I' and end in I or I' . (7.3) shows that as the index set I increases, more trajectories are maintained and the probability of remaining in I increases. (7.5) shows that the probability that the original infinite dimensional system is currently in I must be larger than or equal to the probability that the system has stayed in I for all times, $t \in [t_0, t_f]$.

Now we can apply the FSP algorithm to (2.3) to find a finite ordered index set I that truncates the original infinite state space to a finite state space such that the error

$$\|P^I(S, t) - P_I(S, t)\| \leq \delta.$$

** The Finite State Projection Algorithm*

Step 0.

Choose the final time of interest, t_f .

Specify the acceptable error, $\delta > 0$.

Choose an initial finite set of states, I_0 for the FSP.

Initialize a counter, $j = 0$.

Step 1.

Compute $\Gamma_{I_j} = \mathbf{1}^T P^{I_j}(S, t_f) = \mathbf{1}^T \exp(M_{I_j, t_f}) P^{I_j}(S, t_0)$.

Step 2.

If $\Gamma_{I_j} \geq 1 - \delta$: $I = I_j$, Stop.

$P^I(S, t_f)$ approximates $P_I(S, t_f)$ within error δ .

Else: Go to Step 3.

Step 3.

Add more states to I_j and obtain I_{j+1} .

Increment j as $j + 1$ and return to Step 1.

In Step 0, I_0 can be determined based on the initial probability distribution $P(S, t_0)$. In Step 3 of the FSP algorithm, a method to expand I_j to I_{j+1} is not explicitly stated. There may be many methods to expand the state space, and Munsky [11] illustrates one way to perform the expansion, called N -step reachability. Let I_0 be the initial state and define I_j inductively. Let I_{j+1} contain all states in I_j combined with all states which can be reached from I_j in 1 reaction. Then, I_j denotes the set of all states which can be reached from the initial state in j or fewer reactions. This is how the algorithm expands the state space in Step 3. Munsky showed that for sufficiently large j , $\Gamma_{I_j} = \mathbb{1}^T \exp(M_{I_j} t_f) P^{I_j}(S, t_0) \geq 1 - \delta$ is satisfied [11]. In addition, for I that we find in the FSP algorithm, we have that

$$\|P_I(S, t) - P^I(S, t)\| \leq \delta,$$

for $t \in [t_0, t_f]$ is guaranteed.

However, when multiple time scales exist, the FSP algorithm suffers from computational issues for two reasons. First, when the algorithm expands I_j in Step 3, it equally treats the transition rates between states, even though transitions by the fast reactions are much more probable than transitions by the slow reactions. Second, to compute Γ_{I_j} in Step 1, the algorithm has to solve the full CME at $t = t_f$, to obtain $P^{I_j}(S, t_f)$, which contains both slow and fast species. To handle these problems, we propose the EFSP algorithm, when two time-scale exists. In Step 3 of the EFSP algorithm, we aggregate the fast species and apply the N -step reachability to the slow species, by using the fact that transitions by the fast reactions are much more probable than transitions by the slow reactions. In Step 1 of the EFSP algorithm, we use the model reduction technique to approximate the original CME with Σ_{final} , which contains the slow species only, and solve the approximated CME at $t = t_f$.

7.2 The EFSP algorithm where two time-scale exists

Let $I_x = \{i_1, i_2, \dots, i_m\}$ denote a finite ordered index set for the slow species. Then for the given I_x , we can define a truncated finite state space of the slow species, $\Omega_x^{I_x}$, as follows:

$$\Omega_x^{I_x} = \{\mathbf{x}_{i_1}, \mathbf{x}_{i_2}, \dots, \mathbf{x}_{i_m}\}.$$

Based on (5.5), and a given finite ordered index set I_x , we define $\hat{P}^{I_x}(X, t)$ as solutions of

$$\frac{d}{dt} \hat{P}^{I_x}(X, t) = \hat{A}_{I_x} \hat{P}^{I_x}(X, t), \hat{P}^{I_x}(X, t_0) = \hat{P}_{I_x}(X, t_0), \quad (7.6)$$

where $\hat{P}^{I_x}(X, t)$ is the approximated finite dimensional marginal probability distribution of the slow-species counts. In (5.5), $\hat{P}(X, t)$ is an infinite dimensional vector, because Ω_x , the state space of the slow species is infinite. Therefore, we apply the EFSP algorithm to (5.5) to find a finite ordered index set I_x that truncates the infinite state space of the slow species to a finite state space and approximate $\hat{P}(X, t)$ as $\hat{P}^{I_x}(X, t)$ with error δ .

* The Enhanced Finite State Projection Algorithm

Step 0.

Choose the final time of interest, t_f .

Specify the acceptable error, $\delta > 0$.

Choose an initial finite set of states, $I_{x,0}$ for the FSP.

Initialize a counter, $i = 0$.

Step 1.

Compute $\Gamma_{I_{x,i}} = \mathbb{1}^T \hat{P}^{I_{x,i}}(X, t_f) = \mathbb{1}^T \exp(\hat{A}_{I_{x,i}} t_f) \hat{P}^{I_{x,i}}(X, t_0)$.

Step 2.

If $\Gamma_{I_{x,i}} \geq 1 - \delta$: $I_x = I_{x,i}$, Stop.

$\hat{P}^{I_x}(X, t_f)$ approximates $\hat{P}_{I_x}(X, t_f)$ within error δ .

Else: Go to Step 3.

Step 3.

Add more elements to $I_{x,i}$ and obtain $I_{x,i+1}$.

Increment i as $i + 1$ and return to Step 1.

In Step 3 of the EFSP algorithm, a method to expand $I_{x,i}$ to $I_{x,i+1}$ is not explicitly stated. Fig. 7-2 shows a two-dimensional integer lattice when only one species for both slow (X_1) and fast species (Y_1) exist. Based on the fact that moving horizontally (by the fast reactions) is much more probable than moving vertically (by the slow reactions), we aggregate all state, that have the same slow-species counts, as a single state, and apply the N -step reachability procedure to the slow species only. It solves the first computational issue of the original FSP algorithm.

$\hat{P}^{I_{x,i}}(X, t_f)$ in Step 1 of the EFSP algorithm is defined in (7.6). Unlike the original FSP algorithm, which has to calculate original CME that contains both fast and slow species, our algorithm relies on the approximated CME, (7.6), that contains the slow species only. It solves the second computational issue of the original FSP algorithm. To obtain $\hat{P}^{I_{x,i}}(X, t_f)$ at i^{th} iteration, we have to approximate $Y_n(\mathbf{x}, t)$ as $\hat{Y}_n(\mathbf{x})$ for all $\mathbf{x} \in \Omega_x^{I_{x,i}}$. However, $\hat{Y}_n(\mathbf{x})$ for $\mathbf{x} \in \Omega_x^{I_{x,i-1}}$ is already calculated at $(i-1)^{th}$ iteration, so we additionally need to calculate $\hat{Y}_n(\mathbf{x})$ only for $\mathbf{x} \in \Omega_x^{I_{x,i}} \setminus \Omega_x^{I_{x,i-1}}$.

For convenience, let I_x be $\{i_1, \dots, i_m\}$, which is the ordered index set for the slow species obtained from the EFSP algorithm. Then,

$$\|\hat{P}_{I_x}(X, t_f) - \hat{P}^{I_x}(X, t_f)\| \leq \delta$$

is satisfied, because we choose I_x that satisfies $\Gamma_{I_x} \geq 1 - \delta$ in Step 2. Furthermore, we can claim that

$$\|\hat{P}_{I_x}(X, t) - \hat{P}^{I_x}(X, t)\| \leq \delta, \quad (7.7)$$

for $t \in [t_0, t_f]$, because we expand our $I_{x,i}$ by using N -step reachability procedure and it guarantees the time extension [11] [12]. Now we can claim the following:

Theorem 7.2.1. *Given $t_f > t_0 > 0$, the approximation error between $P_{I_x}(X, t)$ and $\hat{P}^{I_x}(X, t)$ satisfies*

$$\begin{aligned} & \sup_{t \in [t_0, t_f]} \|P_{I_x}(X, t) - \hat{P}^{I_x}(X, t)\| \\ & \leq k_1 \int_{t_0}^{t_f} \|\exp\{\hat{A}\}(t_f - \tau)\| d\tau \Delta_\varepsilon + O(\varepsilon) + \delta. \end{aligned}$$

In addition, as $\varepsilon \rightarrow 0$, the right-hand side of the above inequality goes to $k\Delta_0 + \delta$, where $k\Delta_0$ is defined in Corollary 6.2.3.

The proof of Theorem 7.2.1 is in the Appendix. Theorem 7.2.1 shows that we approximated original infinite dimensional CME, $P(X, t)$, with an m -dimensional CME that contains the slow species only, $\hat{P}^{l_x}(X, t)$, with the quantifiable error bound. This error becomes smaller as δ or ε decreases. To show the utility of our algorithm, we consider two examples.

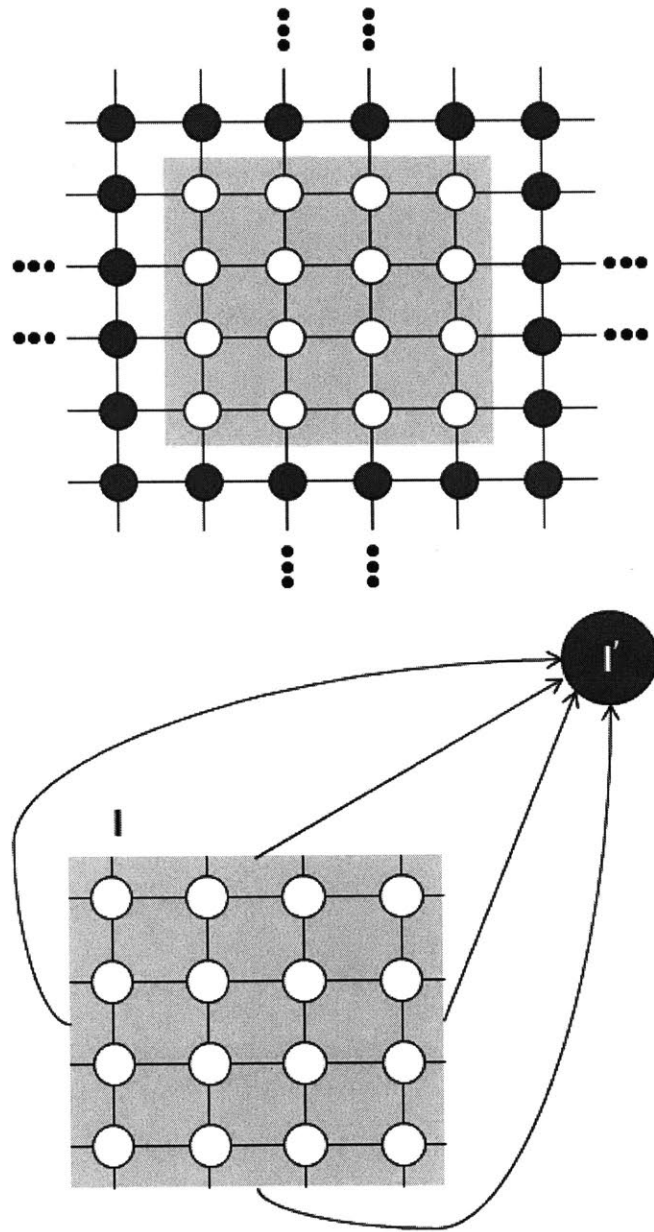


Figure 7-1: Schematic for the FSP algorithm. (Top) Schematic of integer lattice that represents all possible infinitely many states when $r = 2$. (Bottom) A finite truncated state space by a projection of the original infinite state space.

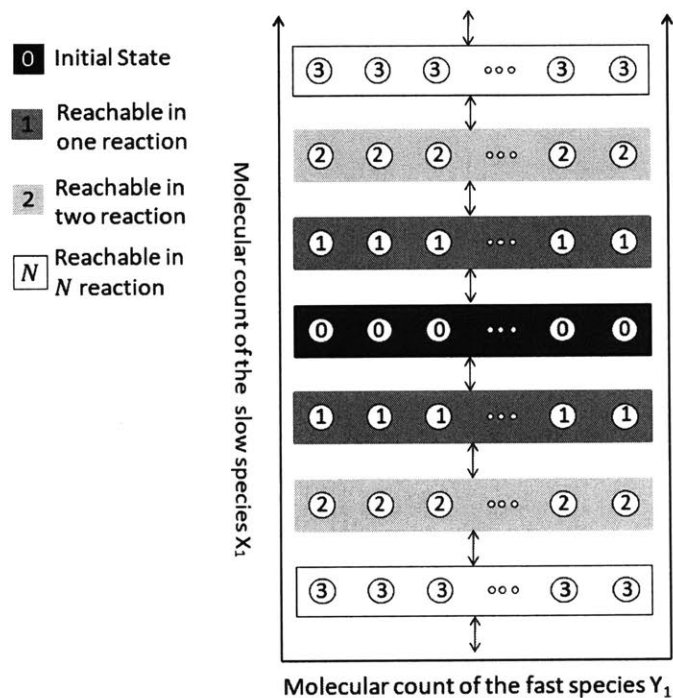


Figure 7-2: Schematic of N -step reachability when two time-scale exists. Here, we visualize a two dimensional lattice, when one slow species (X_1) and one fast species (Y_1) exist. Based on the fact that moving horizontally is much more probable than moving vertically, we aggregate the fast species and apply the N -step reachability to the slow species.

Chapter 8

Examples

In this section, we consider a protein binding reaction and a toggle switch to show the utility of our method.

8.1 Protein Binding Reaction

In this subsection, we consider a protein binding reaction, shown in Fig. 8-1, where two transcriptional components are interconnected [5][21]. Based on the fact that this network

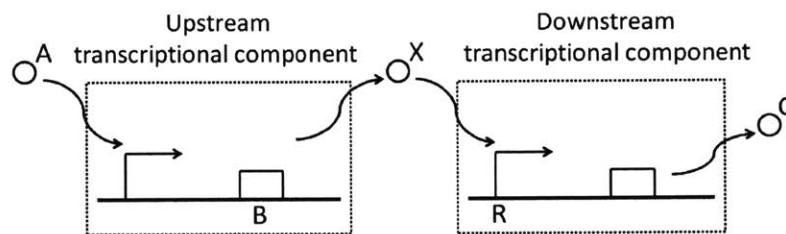


Figure 8-1: The upstream transcriptional component takes protein A as the input and produces protein X as the output. The downstream transcriptional component takes protein X as the input, and X binds with promoter R and produces complex C as the output.

is time-scale separable, the network is analyzed by singular perturbation methods in deterministic models [22]. In Fig. 8-1, the upstream transcriptional component is an input/output system that takes protein A as the input and produces protein X as the output. The downstream transcriptional component takes protein X as the input, and X binds with promoter R and produces complex C as the output. In the upstream transcriptional component, we

let k be the production rate of X and let b be the decay rate of X , including both dilution and degradation. In the downstream transcriptional component, we let a and d be the association and dissociation rate constants of protein X to promoter R . Then we can write the chemical reactions as follows [5]:



In (8.1), there exists a constant R_t that satisfies $R_t = R + C$, because the total concentration of the promoter is conserved. We know that $aR_t, d \gg b, k$, because the protein and the promoter's binding and unbinding reactions are much faster than the protein's decay and production reactions. Therefore, we can divide reactions in two groups: $\emptyset \xrightleftharpoons[b]{k} X$ are two slow reactions and $X + R \xrightleftharpoons[d]{a} C$ are two fast reactions. When we define $X_1 = X + C$, we can find out that X_1 is a slow species and C is a fast species which is bounded by R_t , because count of X_1 is never changed and count of C is changed by the fast reactions. When we define $\varepsilon = \frac{b}{d}$, which satisfies $0 < \varepsilon \ll 1$ and let $k = b$, $aR_t = \frac{d}{2}$, $\mathbf{s} = [x_1, c]^T$, we can derive the following propensity functions and corresponding stoichiometries for both fast and slow reactions as

$$\begin{aligned} a_1(x_1, c) &= b, \gamma_1 = [+1, 0]^T, a_2(x_1, c) = b(x_1 - c), \gamma_2 = [-1, 0]^T, \\ a_3(x_1, c) &= \frac{1}{\varepsilon} \frac{b}{2VR_t} (x_1 - c)(R_t - c), \gamma_3 = [0, +1]^T, \\ a_4(x_1, c) &= \frac{1}{\varepsilon} bc, \gamma_4 = [0, -1]^T, \end{aligned}$$

where, V is the volume.

The state space of the fast species is $\Omega_y = \{0, 1, 2, \dots, R_t\}$, which is a finite set, and the state space of the slow species is $\Omega_x = \{0, 1, 2, \dots\}$ which is an infinite set. Based on the above propensity functions and stoichiometries, for $x_1 \in \Omega_x$ and $c \in \Omega_y$, we can derive the

CME as follows:

$$\begin{aligned}
\frac{d}{dt}P(x_1, c, t) &= -b(x_1 - c)P(x_1, c, t) \\
&- \frac{1}{\varepsilon} \frac{b}{2VR_t} (x_1 - c)(R_t - c)P(x_1, c, t) - \frac{1}{\varepsilon} bcP(x_1, c, t) \\
&- bP(x_1, c, t) + b((x_1 + 1) - c)P(x_1 + 1, c, t) \\
&+ \frac{1}{\varepsilon} \frac{b}{2VR_t} (x_1 - (c - 1))(R_t - (c - 1))P(x_1, c - 1, t) \\
&+ \frac{1}{\varepsilon} b(c + 1)P(x_1, c + 1, t) + bP(x_1 - 1, c, t).
\end{aligned} \tag{8.2}$$

We can check that (8.2) is in (2.5) form. By using (8.2), we can derive ODEs for the slow-species counts' marginal probability distribution as follows:

$$\begin{aligned}
\frac{d}{dt}P(x_1, t) &= -bx_1P(x_1, t) + b(x_1 + 1)P(x_1 + 1, t) \\
&- b\mu_1(x_1 + 1, t)P(x_1 + 1, t) + b\mu_1(x_1, t)P(x_1, t) \\
&- bP(x_1, t) + bP(x_1 - 1, t).
\end{aligned} \tag{8.3}$$

We can check that (8.3) is in (3.3) form. Then, (8.3) can be written as a single linear expression, as in (3.5) form, as follows:

$$\frac{d}{dt}P(X_1, t) = A(Y_2(x_1, t))P(X_1, t), \tag{8.4}$$

where $P(X_1, t)$ is an infinite dimensional vector, and

$$A_{ij} = \begin{cases} -b(x_j - \mu_1(x_j, t)) - b & \text{if } i = j, \\ b(x_j - \mu_1(x_j, t)) & \text{if } i = j - 1, \\ b & \text{if } i = j + 1, \\ 0 & \text{Otherwise.} \end{cases}$$

By using (8.2), we can also derive ODEs for the fast-species counts' first 2 conditional

moments as follows:

$$\begin{aligned}
\varepsilon \frac{d}{dt} Y_2(x_1, t) &= \\
&\left[\begin{array}{cc} -b - \frac{b(x_1 + R_t)}{2VR_t} & \frac{b}{2VR_t} \\ b + \frac{b(2bx_1R_t - bx_1 - bR_t)}{2VR_t} & -2b + \frac{b - 2bx_1 - 2bR_t}{2VR_t} \end{array} \right] Y_2(x_1, t) \\
&+ \begin{bmatrix} \frac{bx_1}{2V} \\ \frac{bx_1}{2V} \end{bmatrix} + \begin{bmatrix} 0 \\ \frac{b}{VR_t} \end{bmatrix} \mu_3(x_1, t) + O(\varepsilon) \\
&= C(x_1)Y_2(x_1, t) + c_1(x_1) + c_2\mu_3(x_1, t) + O(\varepsilon),
\end{aligned} \tag{8.5}$$

which is in (3.8) form. By combining (8.4) and (8.5), we can obtain ODEs in Σ_{true} form. Here, $\mu_3(x_1, t)$ is not a function of $Y_2(x_1, t)$. Therefore, to close the dynamics, we need to approximate $\mu_3(x_1, t)$ as an affine function of $Y_2(x_1, t)$ as follows:

$$\mu_3(x_1, t) \approx \phi(Y_2(x_1, t)) = K_{32}\mu_2(x_1, t) + K_{31}\mu_1(x_1, t) + K_{30}.$$

By solving the linear program in (4.4), we can obtain

$$K_{32} = 15, K_{31} = -56, K_{30} = 30 \text{ and } \rho_2 = 30.$$

When we substitute $\mu_3(x_1, t)$ with $\phi(Y_2(x_1, t))$ in (8.5), we can obtain ODEs in Σ_{closed} form. To approximate $Y_2(x_1, t)$ as functions of the slow-species counts, we let $\varepsilon = 0$ in Σ_{closed} , and obtain

$$\begin{aligned}
C(x_1) \begin{bmatrix} \tilde{\mu}_1^0(x_1) \\ \tilde{\mu}_2^0(x_1) \end{bmatrix} + c_1(x_1) + c_2(K_{32}\tilde{\mu}_2^0(x_1) \\
+ K_{31}\tilde{\mu}_1^0(x_1) + K_{30}) = 0.
\end{aligned} \tag{8.6}$$

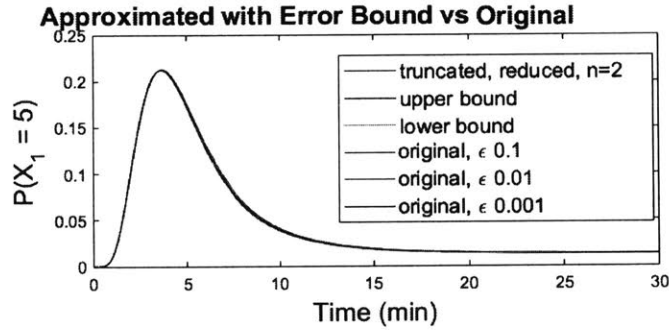
By solving (8.6), we can obtain $\tilde{\mu}_1^0(x_1)$ and $\tilde{\mu}_2^0(x_1)$ as follows:

$$\begin{aligned}
\tilde{\mu}_2^0(x_1) &= K_{21}\tilde{\mu}_1^0(x_1) + K_{20}, \text{ where} \\
K_{20} &= \frac{ax_1R_t + 2aK_{30}}{2aR_t + 2ax_1 - 2aK_{32} - a + 2dV}, \\
K_{21} &= \frac{2ax_1R_t - aR_t - ax_1 + 2aK_{31} + dV}{2aR_t + 2ax_1 - 2aK_{32} - a + 2dV}, \\
\tilde{\mu}_1^0(x_1) &= \frac{aK_{20} + ax_1R_t}{aR_t + ax_1 - aK_{21} + dV}.
\end{aligned} \tag{8.7}$$

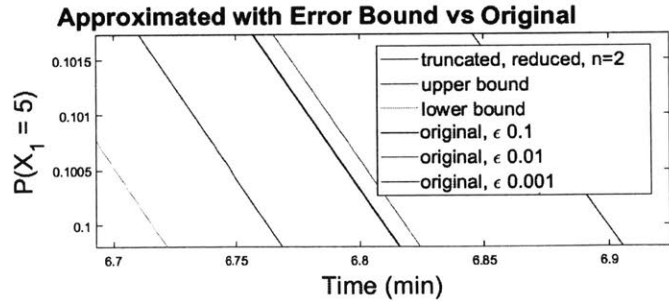
We can obtain the CME with the slow species only, by substituting $\mu_1(x_1, t)$ as $\tilde{\mu}_1^0(x_1)$ in (8.4). Now we should apply the EFSP algorithm to the infinite dimensional approximated CME that contains the slow-species only to find I_x .

When we let $b = 0.4[\text{min}^{-1}]$, $R_t = 10[\text{molecules}]$, $V = 1[\mu\text{m}^3]$, $t_0 = 0[\text{min}]$, $t_f = 30[\text{min}]$, $X_1(t_0) = 10[\text{molecules}]$, $C(t_0) = 2[\text{molecules}]$ and the EFSP error $\delta = 10^{-5}$, we can find $x_{1,max}$, the upperbound of X_1 as 16, by using the EFSP algorithm. This implies we succeed to truncate Ω_x as $\Omega_x^t = \{0, 1, 2, \dots, x_{1,max}\}$, which is a finite set. Furthermore, Δ_0 in Theorem 7.1 can be accomplished at $x_1 = 5$ and $i = 1$, which means $\int_0^\infty \|d_i \exp\{(C(x_1) + c_2 K)t\}\| dt = 0.85$. k_1 in Lemma 6.2 is 0.2, $\|c_2\| = \frac{1}{50}$ and $\|\exp\{\hat{A}(t_f - \tau)\}\| = 0.1 * \exp\{-0.45(t_f - \tau)\}$. We can obtain the error bound for the marginal probability distribution of the slow species in Theorem 7.1 based on these values.

Fig. 8-2(a) compares $P(X_1 = 5)$ of Σ_{true} with $\varepsilon = 0.1, 0.01, 0.001$ and those of Σ_{final} with



(a) Comparing $P(X_1 = 5)$ of Σ_{true} with $\varepsilon = 0.1, 0.01, 0.001$ and those of Σ_{final} with $n = 2$, with the error bound obtained from Theorem 7.1.



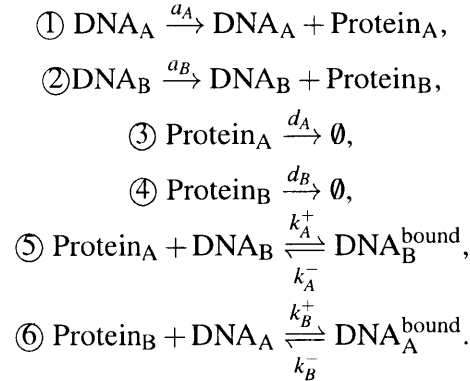
(b) Extended view of the above graph.

Figure 8-2: The slow-species counts' marginal probability distribution, $P(X_1 = 5)$. For this simulation, $\varepsilon = 0.1, 0.01, 0.001$, $n = 2$, $b = 0.4[\text{min}^{-1}]$, $V = 1[\mu\text{m}^3]$, $R_t = 10[\text{molecules}]$ are used.

$n = 2$ and the error bound obtained from Theorem 7.1. Fig. 8-2(b) is the extended view of Fig. 8-2(a). The simulation result shows that $P(X_1 = 5)$ of Σ_{true} with $\varepsilon = 0.001$ is almost the same as those of Σ_{final} , with $n = 2$ and the error bound obtained from Theorem 7.1. Therefore, we can conclude that as $\varepsilon \rightarrow 0$, our approach gives a valid result.

8.2 Toggle Switch

In this subsection, we consider a toggle switch, shown in Fig. 8-3 [5] [23] [24]. Here we consider reciprocal inhibition of two genes A and B , which has been implemented in vivo by Gardner [25]. In Fig. 8-3, DNA_A produces Protein_A with rate a_A . Protein_A can bind (unbind) with DNA_B with rate k_A^+ (k_A^-) and protein-bound DNA stops DNA_B to produce Protein_B . Protein_A decays with rate d_A . The topology is symmetric with A and B , so the same reactions exist for B . Then we can write the chemical reactions for Fig. 8-3 as follows:



Reactions $\textcircled{1}$ and $\textcircled{2}$ correspond to production of protein A and B , from unbound DNA, respectively. Reactions $\textcircled{3}$ and $\textcircled{4}$ describe the decay of proteins. Reactions $\textcircled{5}$ and $\textcircled{6}$ depict binding and unbinding of protein and DNA. Bound DNA loses the ability to produce protein. For convenience, we let $a_A = a_B = a$, $d_A = d_B = d$, $k_A^+ = k_B^+ = k^+$, $k_A^- = k_B^- = k^-$. We point out that $k^+, k^- \gg a, d$ [23]. Then we can divide reactions in two groups: reactions $\textcircled{1}$ to $\textcircled{4}$ are four slow reactions and $\textcircled{5}$ to $\textcircled{6}$ are four fast reactions. In addition, there exists a positive constant D_t that satisfies $\text{DNA}_A + \text{DNA}_A^{\text{bound}} = \text{DNA}_B + \text{DNA}_B^{\text{bound}} = D_t$, due to mass conservation of DNA. When we define $U = \text{Protein}_A - \text{DNA}_B$, $C = \text{Protein}_B - \text{DNA}_A$, $Z = \text{DNA}_A$, $W = \text{DNA}_B$, we can find out that U and C are slow species, and Z and W are

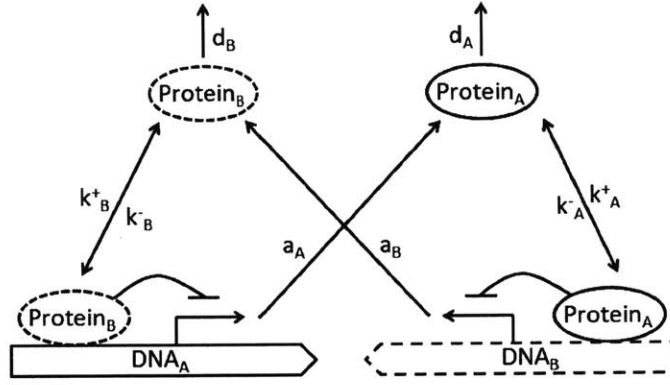


Figure 8-3: Design of a toggle switch. Solid-line species are related to gene A; dashed-line species are related to gene B. Protein_A is produced by DNA_A with rate a_A . It decays with rate d_A and can bind (unbind) DNA_B with rate k_A^+ (k_A^-). Protein-bound DNA stops the protein production. The same reactions exist for B.

fast species that are bounded by D_t . In addition, when we define $\varepsilon = \frac{d}{k^+}$, which satisfies $0 < \varepsilon \ll 1$ and let $k^- = k^+$, $a = \frac{d}{2}$, $\mathbf{s} = [u, c, z, w]^T$, $\mathbf{x} = [u, c]^T$, $\mathbf{y} = [z, w]^T$, we can derive the following propensity functions and corresponding stoichiometries for both fast and slow reactions as

$$\begin{aligned}
 a_1(u, c, z, w) &= \frac{d}{2}z, \gamma_1 = [+1, 0, 0, 0]^T, \\
 a_2(u, c, z, w) &= \frac{d}{2}w, \gamma_2 = [0, +1, 0, 0]^T, \\
 a_3(u, c, z, w) &= d(u + w), \gamma_3 = [-1, 0, 0, 0]^T, \\
 a_4(u, c, z, w) &= d(c + z), \gamma_4 = [0, -1, 0, 0]^T, \\
 a_5(u, c, z, w) &= \frac{1}{\varepsilon} \frac{d}{V} (u + w)w, \gamma_5 = [0, 0, 0, -1]^T, \\
 a_6(u, c, z, w) &= \frac{1}{\varepsilon} d(D_t - w), \gamma_6 = [0, 0, 0, +1]^T, \\
 a_7(u, c, z, w) &= \frac{1}{\varepsilon} \frac{d}{V} (c + z)z, \gamma_7 = [0, 0, -1, 0]^T, \\
 a_8(u, c, z, w) &= \frac{1}{\varepsilon} d(D_t - z), \gamma_8 = [0, 0, +1, 0]^T,
 \end{aligned}$$

where, V is the volume. The state space of the fast species is

$\Omega_y = \{[0; 0], [0; 1], \dots, [0; D_t], \dots, [D_t; 0], [D_t; 1], \dots, [D_t; D_t]\}$, which is a finite set, and the state space of the slow species Ω_x is an infinite set, because species counts of proteins are not bounded. Based on the above propensity functions and stoichiometries, for $(u, c) \in \Omega_x$

and $(z, w) \in \Omega_y$, we can derive the CME as follows:

$$\begin{aligned}
\frac{d}{dt}P(u, c, z, w, t) &= -d\left(\frac{z}{2} + \frac{w}{2} + (u+w) + (c+z)\right) \\
&+ \frac{1}{\varepsilon} \frac{(u+w)w}{V} + \frac{1}{\varepsilon}(D_t - w) + \frac{1}{\varepsilon} \frac{(c+z)z}{V} + \frac{1}{\varepsilon}(D_t - z) \\
P(u, c, z, w, t) &+ 0.5dzP(u-1, c, z, w) + 0.5dwP(u, c-1, z, w) \\
&+ d(u+1+w)P(u+1, c, z, w) + d(c+1+z)P(u, c+1, z, w) \\
&+ \frac{1}{\varepsilon} \frac{d}{V}(u+w+1)(w+1)P(u, c, z, w+1) \\
&+ \frac{1}{\varepsilon} d(D_t - w + 1)P(u, c, z, w-1) \\
&+ \frac{1}{\varepsilon} \frac{d}{V}(c+z+1)(z+1)P(u, c, z+1, w) \\
&+ \frac{1}{\varepsilon} d(D_t - z + 1)P(u, c, z-1, w).
\end{aligned} \tag{8.8}$$

We can check that (8.8) is in (2.5) form. By using (8.8), we can derive ODEs for the slow-species counts' marginal probability distribution as follows:

$$\begin{aligned}
\frac{d}{dt}P(u, c, t) &= -\frac{3}{2}dE(Z+W|u, c)P(u, c, t) - d(u+c)P(u, c, t) \\
&+ \frac{d}{2}E(Z|u-1, c)P(u-1, c, t) + \frac{d}{2}E(W|u, c-1)P(u, c-1) \\
&+ d(u+1)P(u+1, c, t) + d(c+1)P(u, c+1, t) \\
&+ dE(W|u+1, c)P(u+1, c, t) + dE(Z|u, c+1)P(u, c+1, t).
\end{aligned} \tag{8.9}$$

We can check that (8.9) is in (3.3) form. Then, (8.9) can be written as a single linear expression, as in (3.5) form, as follows:

$$\frac{d}{dt}P(X, t) = A(Y_2(\mathbf{x}, t))P(X, t). \tag{8.10}$$

By using (8.8), we can also derive ODEs for the fast-species counts' first 1 conditional

moments as follows:

$$\begin{aligned}
\varepsilon \frac{d}{dt} Y_1(u, c, t) &= \begin{bmatrix} -\frac{d}{V}c - d & 0 \\ 0 & -\frac{d}{V}u - d \end{bmatrix} Y_1(u, c, t) + \begin{bmatrix} dD_t \\ dD_t \end{bmatrix} \\
&- \frac{d}{V} \begin{bmatrix} E(Z^2|u, c) \\ E(W^2|u, c) \end{bmatrix} + O(\varepsilon) \\
&= C(u, c)Y_1(u, c, t) + c_1(u, c) + c_2\mu_2(u, c, t) + O(\varepsilon).
\end{aligned} \tag{8.11}$$

By combining (8.10) and (8.11), we can obtain equations in Σ_{true} form. In Σ_{true} , $\mu_2(u, c, t)$ is not a function of $Y_1(u, c, t)$. Therefore, to close the dynamics, we need to approximate $\mu_2(u, c, t)$ as an affine function of $Y_1(u, c, t)$ as follows:

$$\mu_2(u, c, t) \approx \phi(Y_1(u, c, t)) = K\mu_1(u, c, t) + K_0.$$

By solving the linear program in Eq. (19), we can obtain

$$K = \begin{bmatrix} 0.75 & 0 \\ 0.5 & 0.5 \\ 0 & 0.75 \end{bmatrix}, K_0 = \begin{bmatrix} 0 \\ -0.25 \\ 0 \end{bmatrix} \text{ and } \rho_1 = 0.25.$$

When we substitute $\mu_2(u, c, t)$ with $\phi(Y_1(u, c, t))$ in (8.11), we can obtain our dynamics in Σ_{closed} form. To approximate $Y_1(u, c, t)$ as functions of the slow-species counts, we let $\varepsilon = 0$ in Σ_{closed} and obtain

$$C(u, c)\tilde{\mu}_1^0(u, c) + c_1(u, c) + c_2\phi(\tilde{\mu}_1^0(u, c)) = 0. \tag{8.12}$$

When we solve (8.12), we can obtain $\tilde{\mu}_1^0(u, c)$ as follows:

$$\tilde{\mu}_1^0(u, c) = \begin{bmatrix} \frac{D_t V}{c+0.75+V} \\ \frac{D_t V}{u+0.75+V} \end{bmatrix}.$$

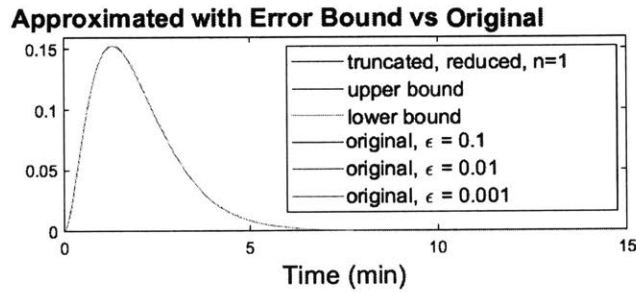
We can obtain the CME with the slow species only, by substituting $\tilde{\mu}_1^\varepsilon(u, c, t)$ as $\tilde{\mu}_1^0(u, c)$ in (8.10). Now we should apply the EFSP algorithm to the infinite dimensional approximated CME that contains the slow-species only to find I_x .

When we let $d = 0.1[\text{min}^{-1}]$, $D_t = 1[\text{molecules}]$, $V = 1[\mu\text{m}^3]$, $t_f = 15[\text{min}]$, $X(0) =$

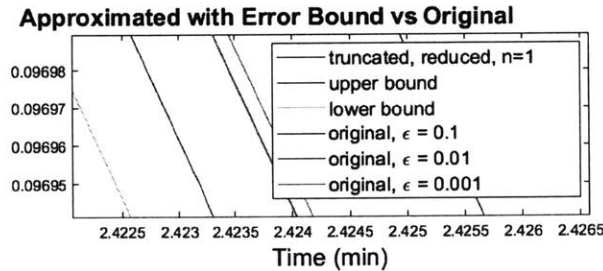
$Y(0) = 8$ [molecules] and the FSP approximation error $\delta = 10^{-6}$, we can find u_{\max} and c_{\max} , the upperbound of U and C as 10 for both of them. This implies that we succeed to truncate Ω_x to

$$\begin{aligned} \Omega_x^{I_x} = \{ & [-D_t; -D_t], [-D_t; -D_t + 1], \dots, [-D_t; -D_t + c_{\max}], \\ & \dots, [-D_t + u_{\max}; -D_t], [-D_t + u_{\max}; -D_t + 1], \\ & \dots, [-D_t + u_{\max}; -D_t + c_{\max}], \end{aligned}$$

which is a finite set. Fig. 8-4(a) compares $P(U = 7, C = 7)$ of Σ_{true} with $\epsilon = 0.1, 0.01, 0.001$



(a) Comparing $P(U = 7, C = 7)$ of Σ_{true} with $\epsilon = 0.1, 0.01, 0.001$ and those of Σ_{final} with $n = 1$, with the error bound obtained from Theorem 7.2.1.



(b) Extended view of the above graph.

Figure 8-4: The marginal probability distribution of the slow-species counts, $P(U = 7, C = 7)$. For this simulation, $\epsilon = 0.1, 0.01, 0.001$, $n = 1$, $d = 0.1$ [min^{-1}], $V = 1$ [μm^3] are used.

and those of Σ_{final} with $n = 1$ and the error bound obtained from Theorem 7.2.1. Fig. 8-4(b) is the extended view of Fig. 8-4(a). The simulation result shows that $P(U = 7, C = 7)$ of Σ_{true} with $\epsilon = 0.001$ is almost the same as those of Σ_{final} , with $n = 1$ and the error bound obtained from Theorem 7.2.1. Therefore, we can conclude that as $\epsilon \rightarrow 0$, our approach gives a valid result.

Chapter 9

conclusion

In this paper, we propose the EFSP algorithm by combining the FSP algorithm and the model reduction technique that we developed. By using the EFSP algorithm, we approximated the infinite dimensional CME as a finite dimensional CME that describes the dynamics of the slow species only. In addition, we quantified the approximation error bound. Our method can be useful for the analysis and design of biomolecular systems. Here are some limitations of our work. First, the conditional moment closure technique does not guarantee $C(\mathbf{x}) + c_2K$ as a stable matrix. Second, we should assume that the number of fast-species counts is bounded. For the future work, we will develop a moment closure technique which can handle these two limitations.

Chapter 10

APPENDIX

10.1 Proof of Proposition 3.0.1 and 3.0.2

ODEs of the slow-species counts' marginal probability distribution can be derived as

$$\begin{aligned}
 \frac{d}{dt}P(\mathbf{x}, t) &= \frac{d}{dt} \sum_{\mathbf{y} \in \Omega_{\mathbf{y}}} P(\mathbf{x}, \mathbf{y}, t) = \sum_{k=1}^{K_s} \sum_{\mathbf{y} \in \Omega_{\mathbf{y}}} [-a_k(\mathbf{x}, \mathbf{y})P(\mathbf{x}, \mathbf{y}) \\
 &\quad + a_k(\mathbf{x} - \gamma_{x,k}, \mathbf{y} - \gamma_{y,k})P(\mathbf{x} - \gamma_{x,k}, \mathbf{y} - \gamma_{y,k})] \\
 &= \sum_{k=1}^{K_s} [-\mathbb{E}[a_k(\mathbf{x}, \mathbf{y})|\mathbf{x}]P(\mathbf{x}, t) \\
 &\quad + \mathbb{E}[a_k(\mathbf{x} - \gamma_{x,k}, \mathbf{y})|\mathbf{x}_i - \gamma_{x,k}]P(\mathbf{x} - \gamma_{x,k}, t)],
 \end{aligned}$$

which is the same as Proposition 3.0.1.

ODEs of the fast-species counts' conditional probability distribution are derived by Gomez[9] as

$$\begin{aligned}
 \varepsilon \frac{d}{dt}P(\mathbf{y}, t|\mathbf{x}) &= \sum_{k=K_s+1}^K (-\varepsilon a_k(\mathbf{x}, \mathbf{y})P(\mathbf{y}, t|\mathbf{x}) \\
 &\quad + \varepsilon a_k(\mathbf{x}, \mathbf{y} - \gamma_{y,k})P(\mathbf{y} - \gamma_{y,k}|\mathbf{x}) + \varepsilon G_1(t)
 \end{aligned} \tag{10.1}$$

where $G_1(t)$ is bounded. Therefore, from (10.1), we can derive

$$\begin{aligned}
 \varepsilon \frac{d}{dt}\mu_w(\mathbf{x}, t) &= \sum_{\mathbf{y} \in \mathbb{Z}^m} \sum_{k=K_s+1}^K [(\Psi_w(\mathbf{y} + \gamma_{y,k}) - \Psi_w(\mathbf{y})) \\
 \varepsilon a_k(\mathbf{x}, \mathbf{y})P(\mathbf{y}, t|\mathbf{x})] + \varepsilon G_2(t) &= \sum_{\mathbf{y} \in \mathbb{Z}^m} \sum_{k=K_s+1}^K [(\Psi_w(\mathbf{y} + \gamma_{y,k}) \\
 - \Psi_w(\mathbf{y})) & (b_k(\mathbf{x}) + c_k(\mathbf{x})\Psi_1(\mathbf{y}) + d_k\Psi_2(\mathbf{y}))] + \varepsilon G_2(t)
 \end{aligned} \tag{10.2}$$

for $1 \leq w \leq n$. Order of $\Psi_w(\mathbf{y} + \gamma_{y,k}) - \Psi_w(\mathbf{y})$ is $w - 1$, so order of the right-hand side of (10.2) returns at most $(w + 1)^{th}$ conditional moments. When we consider w from 1 to n , we can obtain ODEs of the conditional moments of the fast-species counts in Proposition 3.0.2, where $C(\mathbf{x})$, $c_1(\mathbf{x})$ and c_2 are implicitly defined.

10.2 Iterative algorithm in Remark 4.0.1

First we solve (4.4) and let $K = K^*$ be its optimal solution. Then, we will find $K_{(1)}$ such that it is close to K^* but also makes $C(\mathbf{x}) + c_2 K_{(1)}$ stable. To do this, we will find matrices Z and $P_{(1)}$ such that $K_{(1)} = ZP_{(1)}^{-1}$ where Z and $P_{(1)}$ can be obtained by solving

$$\begin{aligned} & \min_{Z, P_{(1)}, \alpha_{(1)}} \|Z - K^* P_{(1)}\|, \\ \text{s.t. } & C(\mathbf{x})P_{(1)} + c_2 Z + (C(\mathbf{x})P_{(1)} + c_2 Z)^T \prec -\alpha_{(1)}I, \\ & P_{(1)} \succ 0, \alpha_{(1)} > 0. \end{aligned}$$

Then, at each iteration, given $P_{(j)}$ and $\alpha_{(j)}$, we first find $K_{(j+1)}$ by solving

$$\begin{aligned} & \min_{K_0, K_{(j+1)}, \gamma} \gamma \\ \text{s.t. } & -\gamma 1^T \leq \mathcal{R}[H_n - (K_{(j+1)}V_n + K_0 1^T)]_i \leq \gamma 1^T, \\ & [C(\mathbf{x}) + c_2 K_{(j+1)}]P_{(j)} + P_{(j)}^T [C(\mathbf{x}) + c_2 K_{(j+1)}]^T \prec -\frac{1}{\alpha_{(j)}}I, \end{aligned}$$

for $i = 1, 2, \dots, m$. Then, given $K_{(j+1)}$, we find $P_{(j+1)}$ and $\alpha_{(j+1)}$ by solving

$$\begin{aligned} & \min_{P_{(j+1)}, \alpha_{(j+1)}} \alpha_{(j+1)} \text{ s.t.} \\ & [C(\mathbf{x}) + c_2 K_{(j+1)}]P_{(j+1)} + P_{(j+1)}^T [C(\mathbf{x}) + c_2 K_{(j+1)}]^T \prec -\alpha_{(j+1)}I, \\ & P_{(j+1)} \succ 0, \alpha_{(j+1)} > 0. \end{aligned}$$

We continue until $\|K_{(j+1)} - K_{(j)}\|$ converges.

10.3 Proof of Theorem 6.1.1

Here, we present the proof of Theorem 6.1.1. We first derive a set of intermediate results, given in Lemma 10.3.1 and 10.3.2, that will be used in the proof.

Lemma 10.3.1. *Given $t_f > t_0 > 0$ and $\mathbf{x} \in \Omega_x$, the approximation error between $\mu_w(\mathbf{x}, t)$ and $\tilde{\mu}_w^\varepsilon(\mathbf{x}, t)$ satisfies*

$$\sup_{t \in [t_0, t_f]} \|\mu_w(\mathbf{x}, t) - \tilde{\mu}_w^\varepsilon(\mathbf{x}, t)\| \leq \int_{t_0}^{t_f} \|f_w \exp\left\{\frac{1}{\varepsilon}(C(\mathbf{x}) + c_2 K)(t_f - \tau)\right\}\| d\tau \frac{\rho_n}{\varepsilon} \|c_2\| = \Delta_{w, \varepsilon}^{\mathbf{x}}.$$

Proof. To quantify the errors, we first define

$$e_1(\mathbf{x}, t) = Y_n(\mathbf{x}, t) - \tilde{Y}_n^\varepsilon(\mathbf{x}, t).$$

Using (3.9) and (4.5), we can derive

$$\begin{aligned} \varepsilon \frac{d}{dt} e_1(\mathbf{x}, t) &= (C(\mathbf{x}) + c_2 K) e_1(\mathbf{x}, t) \\ &+ c_2 (\mu_{n+1}(\mathbf{x}, t) - (KY_n(\mathbf{x}, t) + K_0)), e_1(\mathbf{x}, t_0) = 0. \end{aligned} \tag{10.3}$$

By solving (10.3),

$$\begin{aligned} e_1(\mathbf{x}, t) &= \int_{t_0}^t \exp\left\{\frac{1}{\varepsilon}(C(\mathbf{x}) + c_2 K)(t - \tau)\right\} \\ &\left[\frac{1}{\varepsilon} c_2 (\mu_{n+1}(\mathbf{x}, \tau) - (KY_n(\mathbf{x}, \tau) + K_0))\right] d\tau. \end{aligned} \tag{10.4}$$

Because of Eq (10.4), we can obtain

$$\begin{aligned} \sup_{t \in [t_0, T]} \|\mu_w(\mathbf{x}, t) - \tilde{\mu}_w^\varepsilon(\mathbf{x}, t)\| &= \sup_{t \in [t_0, T]} \|f_w e_1(\mathbf{x}, t)\| \\ &\leq \sup_{t \in [t_0, T]} \int_{t_0}^t \|f_w \exp\left\{\frac{1}{\varepsilon}(C(\mathbf{x}) + c_2 K)(t - \tau)\right\}\| \\ &\left[\frac{1}{\varepsilon} c_2 (\mu_{n+1}(\mathbf{x}, \tau) - (KY_n(\mathbf{x}, \tau) + K_0))\right] d\tau \\ &\leq \sup_{t \in [t_0, T]} \int_{t_0}^t \left[\|f_w \exp\left\{\frac{1}{\varepsilon}(C(\mathbf{x}) + c_2 K)(t - \tau)\right\}\| \right. \\ &\left. \left\|\frac{1}{\varepsilon} c_2 (\mu_{n+1}(\mathbf{x}, \tau) - (KY_n(\mathbf{x}, \tau) + K_0))\right\|\right] d\tau \\ &\leq \int_{t_0}^T \left\|f_w \exp\left\{\frac{1}{\varepsilon}(C(\mathbf{x}) + c_2 K)(T - \tau)\right\}\right\| d\tau \frac{\rho_n}{\varepsilon} \|c_2\| \\ &= \Delta_{w, \varepsilon}^{\mathbf{x}}. \end{aligned} \tag{10.5}$$

□

Lemma 10.3.2. *Given $t_f > t_0 > 0$ and $\mathbf{x} \in \Omega_x$, the approximation error between $\tilde{\mu}_w^\varepsilon(\mathbf{x}, t)$ and $\tilde{\mu}_w^0(\mathbf{x})$ satisfies*

$$\sup_{t \in [t_0, t_f]} \|\tilde{\mu}_w^\varepsilon(\mathbf{x}, t) - \tilde{\mu}_w^0(\mathbf{x})\| \leq \int_{t_0}^{t_f} \|f_w \exp\{\frac{1}{\varepsilon}(C(\mathbf{x}) + c_2K)(t_f - \tau)\}\| \|G(\tau)\| d\tau = O(\varepsilon).$$

Proof. Next we define

$$e_2(\mathbf{x}, t) = \tilde{Y}_n^\varepsilon(\mathbf{x}, t) - \tilde{Y}_n^0(\mathbf{x}).$$

Using (4.5) and (5.1), we can derive

$$\varepsilon \frac{d}{dt} e_2(\mathbf{x}, t) = (C(\mathbf{x}) + c_2K)e_2(\mathbf{x}, t) + \varepsilon G(t), e_2(\mathbf{x}, t_0) = 0. \quad (10.6)$$

By solving (10.6), we can derive

$$e_2(\mathbf{x}, t) = \int_{t_0}^t \exp^{\frac{1}{\varepsilon}(C(\mathbf{x}) + c_2K)(t - \tau)} G(\tau) d\tau. \quad (10.7)$$

Because of (10.7), we can obtain

$$\begin{aligned} \sup_{t \in [t_0, T]} \|\tilde{\mu}_w^\varepsilon(\mathbf{x}, t) - \tilde{\mu}_w^0(\mathbf{x})\| &= \sup_{t \in [t_0, T]} \|f_w e_2(\mathbf{x}, t)\| \\ &= \sup_{t \in [t_0, T]} \left\| \int_{t_0}^t f_w \exp\left\{\frac{1}{\varepsilon}(C(\mathbf{x}) + c_2K)(t - \tau)\right\} G(\tau) d\tau \right\| \\ &\leq \sup_{t \in [t_0, T]} \int_{t_0}^t \left\| f_w \exp\left\{\frac{1}{\varepsilon}(C(\mathbf{x}) + c_2K)(t - \tau)\right\} \right\| \|G(\tau)\| d\tau \\ &= O(\varepsilon). \end{aligned} \quad (10.8)$$

□

The first inequality of Theorem 6.1.1 can be directly obtained by combining Lemmas 10.3.1 and 10.3.2, result of (5.4) and triangular inequality. For the second inequality, Δ_ε can be obtained by

$$\Delta_\varepsilon = \sup_{w \in \{1, 2\}, \mathbf{x} \in \Omega_x} \Delta_{w, \varepsilon}^{\mathbf{x}} + \lambda^{\mathbf{x}}.$$

This completes the proof of Theorem 6.1.1.

10.4 Proof of Lemma 6.2.1

Since $\Delta_1(t) = [A(Y_2(\mathbf{x}, t))] - \hat{A}$, (\bar{i}, \bar{j}) component of $\Delta_1(t)$ can be written as $[\Delta_1(t)]_{\bar{i}\bar{j}} = c_k(\mathbf{x}_{i_{\bar{j}}})(\mu_1(\mathbf{x}_{i_{\bar{j}}}, t) - \hat{\mu}_1(\mathbf{x}_{i_{\bar{j}}})) + d_k(\mu_2(\mathbf{x}_{i_{\bar{j}}}, t) - \hat{\mu}_2(\mathbf{x}_{i_{\bar{j}}}))$, which is bounded by $(\|c_k(\mathbf{x}_{i_{\bar{j}}}\| + \|d_k\|)\Delta_\varepsilon + O(\varepsilon))$. Therefore, k_1 can be obtained as

$$k_1 = \sup_{k, \bar{j}} (\|c_k(\mathbf{x}_{i_{\bar{j}}}\| + \|d_k\|).$$

10.5 Proof of Theorem 6.2.2

We define

$$e_3(t) = P(X, t) - \hat{P}(X, t).$$

Then, we can derive

$$\frac{d}{dt}e_3(t) = \hat{A}e_3(t) + \Delta_1(t)P(X, t) = \hat{A}e_3 + w(t), e_3(t_0) = 0, \quad (10.9)$$

using (5.5) and (6.1). By solving (10.9), we obtain

$$e_3(t) = \int_{t_0}^t \exp\{\hat{A}(t - \tau)\} w(\tau) d\tau. \quad (10.10)$$

Here, the norm of $w(t)$ is bounded by

$$\|w(t)\| = \|\Delta_1(t)P(X, t)\| \leq \|\Delta_1(t)\|_{l_1 - l_\infty} \leq k_1 \Delta_\varepsilon + O(\varepsilon) \quad (10.11)$$

By combining (10.10) and (10.11), we can derive

$$\begin{aligned} \sup_{t \in [t_0, t_f]} \|e_3(t)\| &= \sup_{t \in [t_0, t_f]} \left\| \int_{t_0}^t \exp\{\hat{A}(t - \tau)\} w(\tau) d\tau \right\| \\ &\leq \sup_{t \in [t_0, t_f]} \int_{t_0}^t \|\exp\{\hat{A}(t - \tau)\} w(\tau)\| d\tau \\ &\leq \sup_{t \in [t_0, t_f]} \int_{t_0}^t \|\exp\{\hat{A}(t - \tau)\}\| \|w(\tau)\| d\tau \\ &\leq k_1 \sup_{t \in [t_0, t_f]} \int_{t_0}^t \|\exp\{\hat{A}(t - \tau)\}\| d\tau \Delta_\varepsilon + O(\varepsilon). \end{aligned} \quad (10.12)$$

This completes the proof of Theorem 6.2.2.

10.6 Proof of Corollary 6.2.3

We can obtain

$$\lim_{\varepsilon \rightarrow 0} \Delta_{w,\varepsilon}^{\mathbf{x}} = \int_0^\infty \|f_w \exp\{(C(\mathbf{x}) + c_2 K)t\}\| dt \rho_n \|c_2\|.$$

by substituting $\frac{T-\tau}{\varepsilon}$ for t in Lemma 9.1. This completes the proof of Corollary 6.4

10.7 Proof of Theorem 7.2.1

To prove Theorem 7.2.1, we can combine Theorem 6.2.2, (7.7) and triangular inequality as follows:

$$\begin{aligned} \|P_{I_x}(X,t) - \hat{P}^{I_x}(X,t)\| &\leq \|P_{I_x}(X,t) - \hat{P}_{I_x}(X,t)\| + \|\hat{P}_{I_x}(X,t) - \hat{P}^{I_x}(X,t)\| \leq \\ &\|P(X,t) - \hat{P}(X,t)\| + \delta \leq k_1 \int_{t_0}^{t_f} \|\exp\{\hat{A}\}(t_f - \tau)\| d\tau \Delta_\varepsilon + O(\varepsilon) + \delta. \end{aligned}$$

This completes the proof of Theorem 7.2.1.

Bibliography

- [1] I. Oppenheim, K. Shuler, and G. Weiss *The Journal of Chemical Physics*, vol. 50, no. 1, pp. 460–466, 1969.
- [2] J. L. Spudich and D. E. Koshland Jr *Nature*, vol. 262, no. 5568, p. 467, 1976.
- [3] M. D. Levin, C. J. Morton-Firth, W. N. Abouhamad, R. B. Bourret, and D. Bray *Biophysical journal*, vol. 74, no. 1, pp. 175–181, 1998.
- [4] C. J. Morton-Firth and D. Bray *Journal of Theoretical Biology*, vol. 192, no. 1, pp. 117–128, 1998.
- [5] D. Del Vecchio and R. M. Murray, *Biomolecular feedback systems*. Princeton University Press Princeton, NJ, 2015.
- [6] D. T. Gillespie *The journal of physical chemistry*, vol. 81, no. 25, pp. 2340–2361, 1977.
- [7] C. V. Rao and A. P. Arkin *The Journal of chemical physics*, vol. 118, no. 11, pp. 4999–5010, 2003.
- [8] E. L. Haseltine and J. B. Rawlings *The Journal of chemical physics*, vol. 117, no. 15, pp. 6959–6969, 2002.
- [9] C. A. Gómez-Uribe, G. C. Verghese, and A. R. Tzafriri *The Journal of chemical physics*, vol. 129, no. 24, p. 244112, 2008.
- [10] G. G. Yin and Q. Zhang, *Continuous-time Markov chains and applications: A two-time-scale approach*, vol. 37. Springer Science & Business Media, 2012.

- [11] B. Munsky and M. Khammash *The Journal of chemical physics*, vol. 124, no. 4, p. 044104, 2006.
- [12] S. Peleš, B. Munsky, and M. Khammash *The Journal of chemical physics*, vol. 125, no. 20, p. 204104, 2006.
- [13] H. K. Khalil, “Nonlinear systems,” *Prentice-Hall, New Jersey*, vol. 2, no. 5, pp. 5–1, 1996.
- [14] U. Kwon, M. Naghnaeian, and D. Del Vecchio 2019.
- [15] M. Naghnaeian and D. Del Vecchio in *Control Technology and Applications (CCTA), 2017 IEEE Conference on*, pp. 967–972, IEEE, 2017.
- [16] D. T. Gillespie *Physica A: Statistical Mechanics and its Applications*, vol. 188, no. 1-3, pp. 404–425, 1992.
- [17] N. Herath and D. Del Vecchio *The Journal of Chemical Physics*, vol. 148, no. 9, p. 094108, 2018.
- [18] S. Jayanthi and D. Del Vecchio *IEEE Transactions on Automatic Control*, vol. 56, no. 4, pp. 748–761, 2011.
- [19] M.-N. Contou-Carrere, V. Sotiropoulos, Y. N. Kaznessis, and P. Daoutidis *Systems & Control Letters*, vol. 60, no. 1, pp. 75–86, 2011.
- [20] W. Mitkowski *Technical Sciences*, vol. 56, no. 4, pp. 309–312, 2008.
- [21] U. Alon, *An introduction to systems biology: design principles of biological circuits*. Chapman and Hall/CRC, 2006.
- [22] D. Del Vecchio, A. J. Ninfa, and E. D. Sontag *Molecular systems biology*, vol. 4, no. 1, p. 161, 2008.
- [23] M. Strasser, F. J. Theis, and C. Marr *Biophysical journal*, vol. 102, no. 1, pp. 19–29, 2012.

[24] A. Loinger, A. Lipshtat, N. Q. Balaban, and O. Biham *Physical Review E*, vol. 75, no. 2, p. 021904, 2007.

[25] T. S. Gardner, C. R. Cantor, and J. J. Collins *Nature*, vol. 403, no. 6767, p. 339, 2000.